Methods for Post-Construction Evaluation of Horizontal Directional Drilled Utilities

---

A Thesis

Presented to

the faculty of the School of Engineering and Applied Science

University of Virginia

---

in partial fulfillment

of the requirements for the degree

Master of Science

by

Frank P. Morris, Jr.

May

2014

APPROVAL SHEET

The thesis

is submitted in partial fulfillment of the requirements

for the degree of

Master of Science

(signature)

AUTHOR

The thesis has been read and approved by the examining committee:

Dr. Lindsay Ivey Burden

Advisor

Dr. Andres Clarens

Dr. Brian Smith

Dr. Edward Hoppe

Accepted for the School of Engineering and Applied Science:

(signature)

Dean, School of Engineering and Applied Science

May
2014

2

ABSTRACT:

Trenchless Technology has become an increasingly popular underground utility construction method, beginning in the early 1900s with pipe jacking beneath railroad lines. One method, horizontal directional drilling (HDD), became more common in the 1990s and into the current day. Since trenchless construction does not require an open cut or excavation, cave-in(s), that are potentially dangerous for workers, do not occur. In addition, conduits and utilities can be installed beneath existing structures and roadways without having to demolish current infrastructure. However, the utilization of HDD is associated with the potential risk for ground subsidence and soil heaving. Sinkholes and settlement can form after construction, damaging existing infrastructure and causing safety hazards. Trenchless methods, requiring an annual overcut, disturb soil around the outer diameter of the utility being installed. While the annular overcut is necessary for feeding pipes through the borehole, when used in conjunction with a liquid lubricant, the likelihood for developing voids increases. The annular overcut is also a cause for concern because the consistency and void ratio of the overburden soil change after boring. Inconsistent and void-ridden soil can cause void propagation through the overlying soil until it reaches the surface, where it will become a sinkhole or crack.

This paper addresses post-construction evaluation methods, especially pertaining to the annular space and void propagation region above and around a freshly installed utility in Southern Virginia. Two non-destructive evaluation methods are used to scan the surrounding soil: Ground penetrating-radar (GPR) and FutureScan. FutureScan, a radar device developed by Louisiana Tech University, is capable of being attached to pipe inspection robots and uses a means of penetrating radar to detect voids and inconsistencies in three dimensions. This study examines the difference between GPR and FutureScan, regarding the imaging techniques used and the measured void ratios. All soil conditions for this study pertain to The Virginia Piedmont region.

Relative elevations were recorded before, during, and after drilling, to measure surface movement caused by drilling efforts. The relative elevation was also recorded several months after utility installation, so it could be compared on a long-term scale. Long-term results indicate whether or not the imaging techniques imply subsidence in the long-term. After the analysis was conducted using both FutureScan and GPR, representative soil samples of the test site were retrieved and transported to a geotechnical laboratory for further testing. Based on the GPR and FutureScan findings, the utility of the two post-construction evaluation methods was determined. The results were compared to the relative elevations recorded in the field. Void ratio field data and equipment reliability are limited to Virginia's piedmont region.

INTRODUCTION

Background

Post-construction evaluation methods for HDD are not accepted nor are used often in the field of Geotechnical engineering. While HDD construction often leaves voids or soil anomalies, contractors and engineers have no way to determine the damage. Two technologies, FutureScan and GPR, are potential means of evaluation and will be the focus of this study. It is important to understand the reasoning behind the decision to use HDD construction as opposed to conventional trenching methods. Applications will be described in the following section.

HDD is one of many trenchless utility installation methods; this study focuses on a single method but is not limited to HDD. The HDD process consists of 3 phases: drilling a pilot hole, reaming the pilot hole with a larger diameter cutting bit, casing/utility installation. Once the hole has been completely reamed, the casing or utility is ready to be pulled through the borehole, which is supported by the entrapped slurry (Iseley & Gokhale, 1997). Pipe ramming, microtunneling, pipe jacking are alternative methods. Pipe ramming includes driving a steel casing for the desired utility, which is rammed using dynamic energy from a drive shaft to a reception shaft (Iseley & Gokhale, 1997). Microtunneling is a jacking method, which holds the outer borehole walls open by hydraulic or auger means (Iseley & Gokhale, 1997). Pipe jacking is a manual or mechanical process in which spoils are removed from the inside of the utility (Iseley & Gokhale, 1997). Pipe jacking, similar pipe ramming, also includes drive shaft to reception shaft force to install the utility. Alternative trenchless methods still disturb soil to some degree; therefore, this study is not limited to a single method.

HDD utility installation methods preserve existing infrastructure by having the capability to pitch below roadways. The drill path begins at a downward angle, so drilling can take place beneath existing facilities. Such construction is useful in eliminating open trench cuts, which mitigate roadway traffic, lane closures, and potential detouring. A general overview of HDD construction and methodology is to follow this section.

The first step in HDD construction entails drilling a pilot hole. It is imperative that the correct pitch is made while drilling the pilot hole, for the centerline of the larger bit will naturally follow the pilot hole. Normally, an excavation is made on the opposing end of the drill path. The excavation is often referred to as the receiving pit (Hashash and Javier, 2011). The receiving pit is necessary for pumping soil cuttings produced during drilling. The pit also allows for the utility to slide easily into the future hollowed hole. Initial advancements are performed with a smaller conic-shaped drilling bit, ranging from 3-inches to 6-inches in diameter. Additional drilling rods are stored on the drill rig so that sections may be added as drilling continues. Normally, rod sections are 10-feet long; therefore, a new section is added every 10-feet of drill length. Please refer to Figure 1 for the first step in drilling.
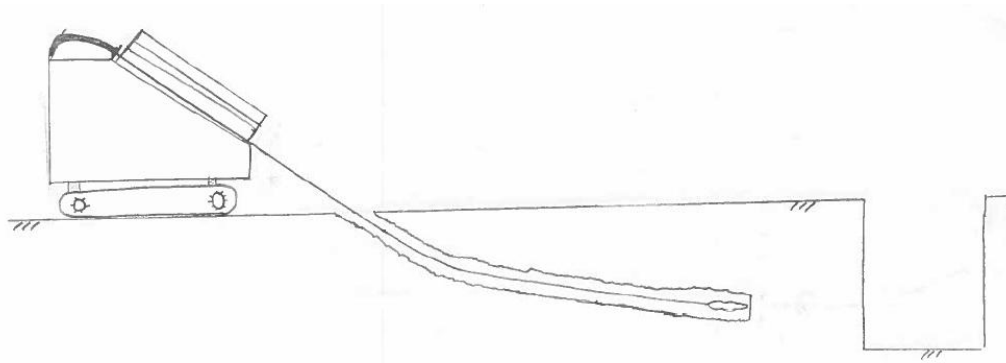
Figure 1. Drilling of the Pilot Hole.

Once the pilot hole reaches the excavation on the opposing end, the small bit is removed, and a large auger bit is attached to the rods. The large auger bit normally has small weep holes in the center, allowing bentonite slurry to be pumped into the borehole. Bentonite slurry is a mixture of water and calcium or sodium bentonite, necessary for lubricating the drill hole and reducing potential swell of the borehole. The slurry is mixed thoroughly in a separate tank and pumped to the hosing at the back of the rig. The slurry then travels through the center of the hollow drilling rods, exiting through the weep holes in the auger bit. As the auger bit turns, the bentonite slurry is flung out from the weep holes and onto the outer walls of the borehole. Simultaneously, the cutting teeth on the auger bit tear through soil, reaming a borehole. Figure 2 is a depiction of the large auger bit releasing bentonite slurry from its weep holes as rod rotation occurs.

Figure 2. Bentonite Slurry being released from the large auger bit (Photo by Frank Morris).

Generally, the back ream (large auger bit) diameter is 1.5 times the diameter of the pipe being installed (Hashash and Javier, 2011). The larger ream accounts for swell of the soil and varying angles of pitch. As the drill rig turns the rods, the bentonite slurry is pumped out of the weep holes in all directions, cutting the soil easily. This step of the drilling process follows the pilot hole back toward the rig as shown in Figure 3.
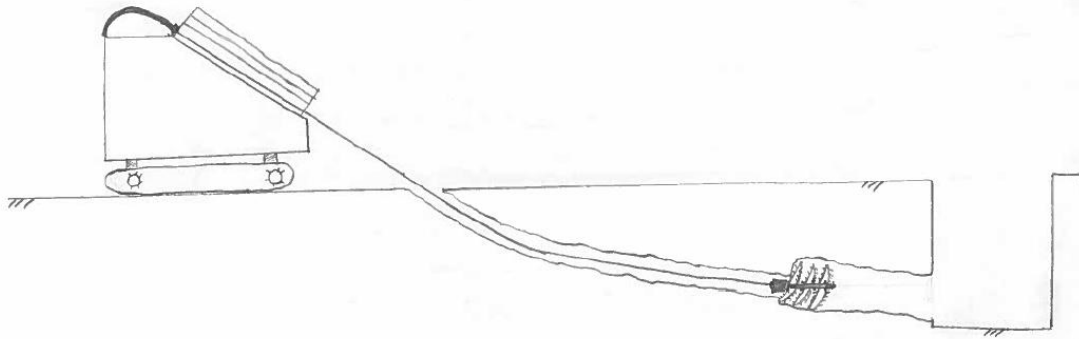
Figure 3. Augering of the larger diameter borehole.

The slurry is pumped out of the excavation as drilling advances. Once the larger diameter auger bit reaches the start, the rig pushes the bit back to the opposing end. During pushing the bit back toward the excavation, slurry is pumped as needed. The pushing further cleans and reams the borehole as displayed in Figure 4.
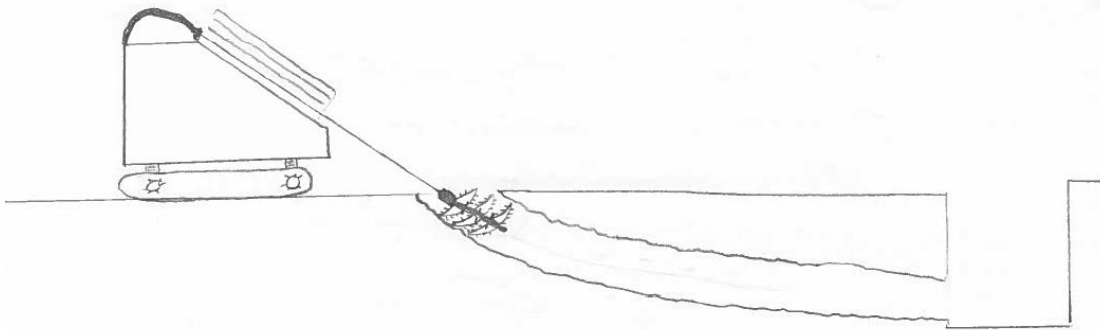

Figure 4. Pushing the large auger bit to the excavation.

Once the large auger bit reaches the opposing end, the bit is then removed from the rods. A spindle is attached to the rod's end, and a fitting plug on the end of the utility is attached to the spindle to keep the open utility from becoming filled with any soil.

Finally, the utility is pulled from the excavation to the initial until it reaches the rig. Please refer to Figure 5 for the last step in HDD construction. Due to the overcut of the back ream, a "filter cake," forms between the outer diameter of the utility and inner borehole walls. The "filter cake," is a mixture of soil cuttings and bentonite, forming around the outer perimeter of the utility. Theoretically, the "filter cake" fills the annular space for the whole length of the borehole. The "filter cake" is variable, for the consistency depends upon soil and bentonite conditions. Oftentimes, engineers call for grouting of the annular space in project specifications. Pumping grout solidifies the annular space, allowing overburden soil stresses to be re-distributed.
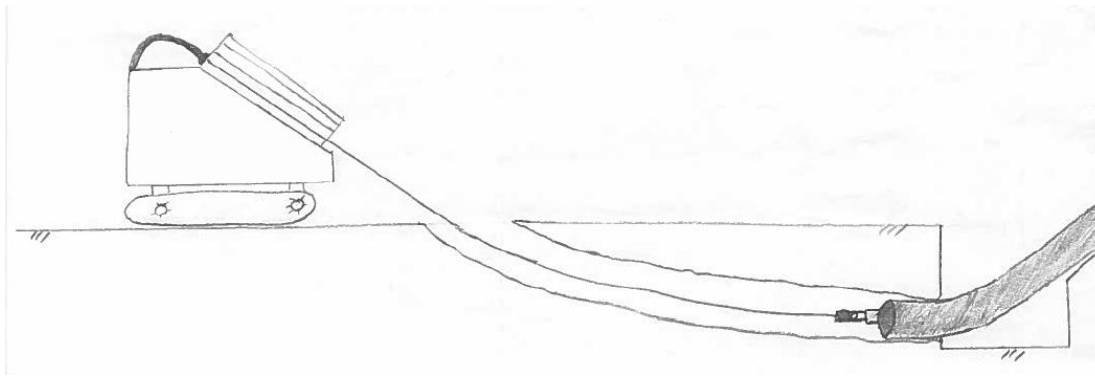
Figure 5. Pulling the utility.

Due to the critical nature of soil beneath existing infrastructure, HDD must be completed carefully. Potential modes of soil failure are as such: settlement, subsidence, heaving, cracking, and hydrofracture. Failure is often due to the annular overcut not being secured. Vertical soil stresses exceed that of the "filter cake" capacity, and collapse of soil into the annular space is likely. Inversely, vertical stresses caused by drilling fluid pressures may be exceeded in the upward direction, causing hydrofracture.

Post-construction evaluation radar scanning methods, GPR and FutureScan, have the potential to determine the consistency of the "filter cake" and sight soil anomalies or voids. Assuming reliability, these methods detect issues prior to damage occurring. The reliability and results of these methods is attempted in conjunction with relative elevation data. Background information on the radar scanning methods will be summarized in the following paragraphs.

GPR is a multi-use technology, developed originally for underground utility and archaeological location. A wheel-mounted GPR has scanning capability that can be performed from the asphalt surface; the machine is rolled along the surface with its scanner flush with existing grades. Results are viewed in top to bottom format. Generally, a 1:1 (inch: foot) ratio is established in the field for scanning anomalies versus depth. GPR is a widely used technology for subterranean location.

FutureScan is a new product, developed by Dr. Erez Allouche from Louisana Tech University. FutureScan is now operated by a closed circuit television video manufacturer and pipe inspector by the name of CUES, Inc. FutureScan, a robot, walks and scans the length of a utility from the inside. Results are viewed in bottom to top format. FutureScan is also wheel-mounted system that contains a front-mounted scanning antenna. The mounted antenna can be turned at various angles so that different viewpoints around the perimeter of the utility may be evaluated. Essentially, a 360-degree inspection of the utility's outer diameter is possible. CUES, Inc. states that FutureScan has the capability to measure 0.5-feet to 3.0-feet beyond the utility's outer diameter, depending upon soil and slurry conditions.

Both scanning devices use the concept of dielectric permittivity to obtain radar gram results, regarding the consistency of the soil. Dielectric constant is a means of

quantifying the consistency or composition of a material. Changes in Dielectric Permittivity (ε) on the radar display indicate differing soil composition. Two charges, positive and negative, are sent into the soil by the machine. The positive charges move forward, while the negative charges are the reflections. Reflections move back toward the voltage source at a certain rate, which is measured by the machine. This rate will indicate material type and composition. Soil anomalies and potential damage will reflect signals at different velocities, relative to undisturbed soil. Such signals will indicate perturbations on the radar gram. Dielectric permittivity is the key to locating such anomalies through radar scanning and can aid in saving existing infrastructure.

Thus far, FutureScan technology offers a more quantitative approach to evaluating voids rather than the current system, which is user specific. Currently, radar scans are analyzed with the naked eye, and results depend upon the experience of the user. Exact measurements of anomalies are scaled at best. GPR results are based on the current analysis system. CUES, Inc. has developed a thorough analysis system based on algorithms and dielectric constants of surrounding soils. The analysis is precise and not based on user interpretation. FutureScan analysis includes drawing lines where scan inversions of frequency or signal velocity occur. Such analysis allows the user to calculate exact volumes of anomalies. If such a system is deemed reliable, then determining remediation steps will be much more efficient.

Ground Penetrating Radar (GPR) is still qualitative, and results depend upon user interpretation. GPR results yield a primitive radar gram with signal inversions that must be scaled. Error exists in the results as well as scaling techniques. Algorithms and thorough analysis based on soil dielectric constant is much more efficient and prevents user error.

The radar scanning used in this project via GPR and FutureScan provide a method through which possible anomalies can be detected post-construction. The dielectric constant is the determining factor of both GPR and FutureScan results. Changes in Dielectric Permittivity (ε) on the radar display indicate voids or soil composition differentiation. Dielectric permittivity is determined by a charge sent through the machine and into the soil. A charge is moved by an energy source, namely voltage (Wightman, Jalinoos, Sirles, and Hanna, 2003). The energy field produces a polarized field, intrinsic polarization, with positive charges moving in the forward direction and negative charges moving in the backward direction (Wightman et al., 2003). Wightman et al. (2003) states: "Permittivity is the primary factor influencing speed of electromagnetic radiation in earth materials at GPR frequencies. Thus, the velocity at which the negative charges reflect back to the antenna is a means of discerning between soil and void." There is a linear relationship between intrinsic polarization (charge) and dielectric permittivity, but dielectric permittivity is often expressed in terms of dielectric constant (K) and permittivity of free space (ε_o):

$$K = \frac{\epsilon}{\epsilon_o}.$$

Once a change a boundary (i.e. anomaly) is reached, a change in dielectric constant is reflected back to the machine through negative charges. Then, an anomaly will be shown on the radar frequency scale. Dielectric constants, for radar frequencies, range from 1 to 80, respectively air to water. So, low dielectric constants, near unity, will imply soil voids.

The site soils for Burnt Chimney and VA-635 are generally classified as Silty-Clayey SANDs and Granites/Gravels, respectively. The site soils are described in the Project and Site Soil Description sections.

The soil types on the sites have known dielectric constants within a specified range. One should expect the Burnt Chimney project site soils to have dielectric constants within the range of 5-to-60. One should expect the VA-635 project site soils to have dielectric constants within the range of 3-to-5. Figure 6 incorporates dielectric constant values as a function of varying soil types, specific to the project sites.
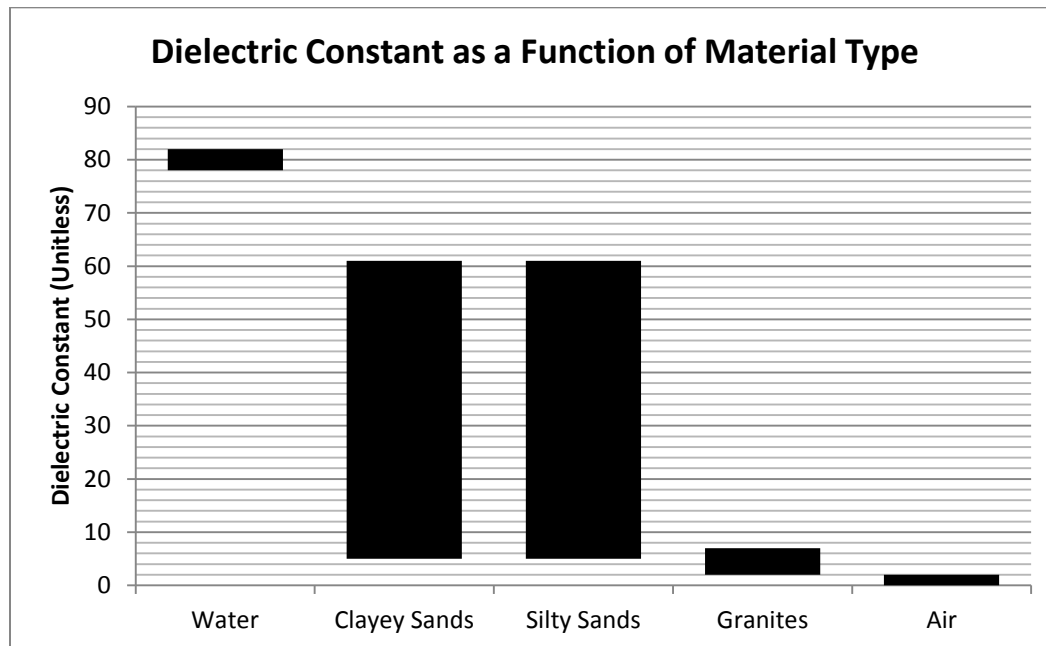

Figure 6. Dielectric Constants and Material Types (Wightman et al., 2003).

Non-destructive evaluation in conjunction with construction can alleviate many of the facility damages that we encounter today using trenchless methods. Radar scanning and dielectric permittivity is the only way to see into the ground without further disturbing soil.

Motivation of Work

Geotechnical engineers need a better means of determining site specific damage. HDD construction leaves an annular cut around the freshly installed utility. In addition, the surrounding ground is disturbed by auguring and drilling fluid pressures.

A certain amount of settlement or upheaval is acceptable, but it would be nice to know how much settlement/upheave will be produced at the time of the site visit. Non-destructive testing methods, FutureScan and GPR, are alternatives to vertical drilling. Although FutureScan and GPR have not been accepted as routine post-construction practice, a case study can prove the reliability of such products. The reliability of these devices has not been established with confidence to date. So, it is important to test GPR and FutureScan for reliability. Scanning results can save infrastructure and lives; therefore, such a study is pertinent. A confident means of determining damage will keep roadways safe.

After drilling and installation using trenchless methods, the risk of ground settlement, subsidence, hydrofracture, or basal upheave is at its' greatest. Previous studies and history indicate that ground disturbance and drilling has damaged existing facilities in the past. Below is an overview of case studies for which failures have occurred.

A case study, that took place in Newton, Illinois by Youssef Hashash and Jamie Javier, displays asphalt failure due to HDD construction. The project site had variable soil conditions: a mix of rock and soft fills. An 18-inch reamer bit drilled the open borehole, and dual 6-inch PVC waterlines were installed. Shortly after construction, heaving of the roadway caused mounding of the surface asphalt. Figure 7 displays the highlighted basal upheave of the roadway, creating bumpy driving conditions. The conditions worsened with a crack in the waterline, and the municipality immediately remediated the roadway with an open-cut trench.

Figure 7. Newton, Illinois HDD Failure (Hashash and Javier, 2011).

A similar case study by Hashash and Javier took place in Salem, Illinois. A steel 8-inch casing was installed beneath an existing roadway using trenchless methods, and cracking of the existing roadway occurred. Moisture, on either side of the cracking, was noted, for drilling fluid was the most likely cause of the surface moisture cracking. Figure 8 depicts longitudinal cracking in the direction of the utility. Hydrofracture is the probable cause of failure in this case. If FutureScan or GPR had been used on the project sites, the infrastructure failures could have been pre-determined, and issues would have been addressed on-site. The radar gram (FutureScan or GPR results) would indicate anomalies in the cracked region. In the

case of the Newton, Illinois project site, FutureScan results would indicate a larger ream-hole diameter than was drilled. In addition, dielectric permittivity values of water may have been sensed close to the ground surface by either device.

Figure 8. Salem, Illinois HDD Failure (Hashash and Jamie Javier, 2011).

FutureScan and GPR, were field tested during a horizontal directional drilling (HDD) project in Southern Virginia. Two additional studies (project sites) were performed on individual sites, characterized by poorly compacted backfill. The goal of this study is to test the reliability of these tools and compare the results to relative elevations (surveys) before, during, and well after reaming a borehole. The reliability of these devices is an important tool for contractors and engineers, for evaluation can be performed at the time of construction. If the results are unfavorable, field changes can be made immediately before the utility or existing facility becomes at risk for failure.

A better means of HDD evaluation is needed so that field changes can be made with confidence. Without reliability and prior experience with GPR and FutureScan, results could mean little. Risk assessment for HDD can be improved, given it often consists of only basic qualitative evaluation (i.e. past experience review); yet, heave risk bears a large influence on HDD market acceptance and growth (J.D. Hair, 1995). Basal upheave is a major concern in HDD practice. Upheave will occur during or after construction, and predicting upheaval prior to construction can be quite difficult. Therefore, non-destructive evaluation is a safe alternative to determining the amount of hydrofracture or borehole expansion after-the-fact. HDD annular void and heave remediation has to occur after construction is complete, regardless of the proposed risk beforehand. Therefore, the post-construction evaluation is a necessary step in verifying the soil (i.e. void) conditions and contractor workmanship before project completion.

GPR and FutureScan can provide insight as to whether to approach remediation, and if so, what types of remediation tactics are necessary. Project remediation, consisting of pressure relief wells and annular space grouting, are post-construction methods. GPR and FutureScan can potentially help the geotechnical engineer and contractor make the decision: whether or not to pursue such remediation. Such technologies, assuming reliability, could save existing infrastructure from damage due to settlement or upheave. One must also take into account fiscal costs, associated with having to

remediate the project site after job completion. GPR and FutureScan could become regular non-destructive testing tools for trenchless utility projects, saving existing infrastructure, time, and money.

Current research expresses the need for such technology; mitigation of upheave and settlement are primary focuses. These sources mention the demand for better methods of trenchless construction verification:

> An important technology ally to HDD contracting is the geotechnical engineer, who stands as the primary independent party most capable of properly assessing HDD feasibility and analyzing HDD behavior for soil heave risk. Therefore, he is also best able to develop compliance documentation, which is the contractors' most reliable tool for prompt payment and dispute resolution. Without a framework of "trust but verify" and compliance transparency now fundamental to public works projects, HDD industry will remain limited by varied instances of sour "black box" experiences and unwelcome surprise claims. (Francis, Kwong, and Kawamura, 2003).

An aid to the geotechnical engineer could be the GPR device on top of a freshly installed utility in combination with the FutureScan robot inside the utility. These devices could add to the technology and assurance of the geotechnical engineer. If GPR and FutureScan prove to be acceptable void detection methods, the "trust but verify" notion can be put to rest. Verification can actually occur, and "black box" experiences and lawsuits can be minimized. These technologies can serve the geotechnical engineer and contractor well. A third party, materials testing firm, can even be used to furnish separate reports based on the contractor's work in accordance with the design specifications.

A comprehensive technical source entitled, "Evaluation of Horizontal Directional Drilling (HDD)", by Youssef Hashash and Jamie Javier describes various state Department of Transportation regulations and procedures when drilling using trenchless methods. Published in 2011, Hashash and Javier list all safe design and construction practices throughout the country. The source does not mention post-construction evaluation. To make HDD a safer practice, reliable post-construction evaluation methods are needed. This recent study does not take into account post-construction evaluation methods, which further supports the need for reliability testing of these products.

More accurate evaluation of hydrofracture risks, is only one step in reducing hydrofracture risks. Coupled with improved evaluation, improvements in management of drilling fluid properties and drilling methods are needed (Bennett, 2009). Hydrofracture is caused by drilling fluid pressures exceeding soil pressure from the annular cut. Fracturing of the soil actually occurs, and drilling fluid can readily flow through the cracks (Gelinas and Mathy, 2004). Such phenomena can cause weak points or fissure cracking within soil beneath existing infrastructure, eventually leading to settlements or upheaval. Drilling fluid may even reach existing grades during construction. Hydrofracture only occurs prior to the soil's plastic

yielding point (Bennett, 2009). FutureScan and GPR can potentially reflect non-homogenous changes in annular cuts, which would indicate hydrofracture potential. FutureScan can be sent down a wet borehole to identify hydrofracture cracking, for the device has waterproof capability. An increasing annular cut would indicate linear strain within soil, and FutureScan has the capability to detect void increases. Regardless, Bennett mentions the need for improvement in permitting, regulatory oversight, and improved evaluation. These non-destructive testing technologies can help all three of Bennett's suggestions by ensuring the proper design and construction methods are used during and after utility installation.

The results from this study could be used to assist engineers and contractors in the prediction of long-term conditions. For instance, if the predictions are unfavorable shortly after construction, then remediation can be performed immediately on-site to ensure existing infrastructure is kept safe.

Previous Studies/ Literature Review

FutureScan was recently developed by Louisiana Tech University engineers. Reliability is still undetermined due to its' recent creation. No papers based on the technology's reliability have been published to date. This serves as a catalyst for more work on the subject. This paper is the first published, regarding FutureScan's reliability and evaluation capability of soil anomalies.

Ground Penetrating Radar (GPR) has been used to locate subterranean voids from the ground surface. Larger voids are capable of being measured using this type of system. The following case study outlines GPR void detection capability.

The Texas Department of transportation used GPR technologies to locate voids and reduce further damage to existing facilities. GPR was successful in locating a 1,080 cubic-foot void beneath U.S. 290 near Austin, Texas (Chen, 2010). A section of U.S. 290, southwest of Austin, was built on top of an MSE (Mechanically-Stabilized Earth Wall). An underground drain pipe, spanning longitudinal (parallel) to lanes, broke at a joint, causing soil fines to wash out of the pipe itself. Thus, a large void formed below the roadway surface. Subsidence and cracking at the surface indicated soil failure below existing grades. Settlements of up to 3-inches were observed. Figure 9 displays the large subsidence between traffic lanes.

Figure 9. Settlement of the Roadway (Chen, 2010).

After evaluating the site using a 400 Megahertz antenna GPR system, an inversion of voltage was noticed on the radar gram in Figure 10 (Chen, 2010). The void dimensions were listed as such: 6 feet deep, 15 feet long, and 12 feet wide (Chen, 2010).
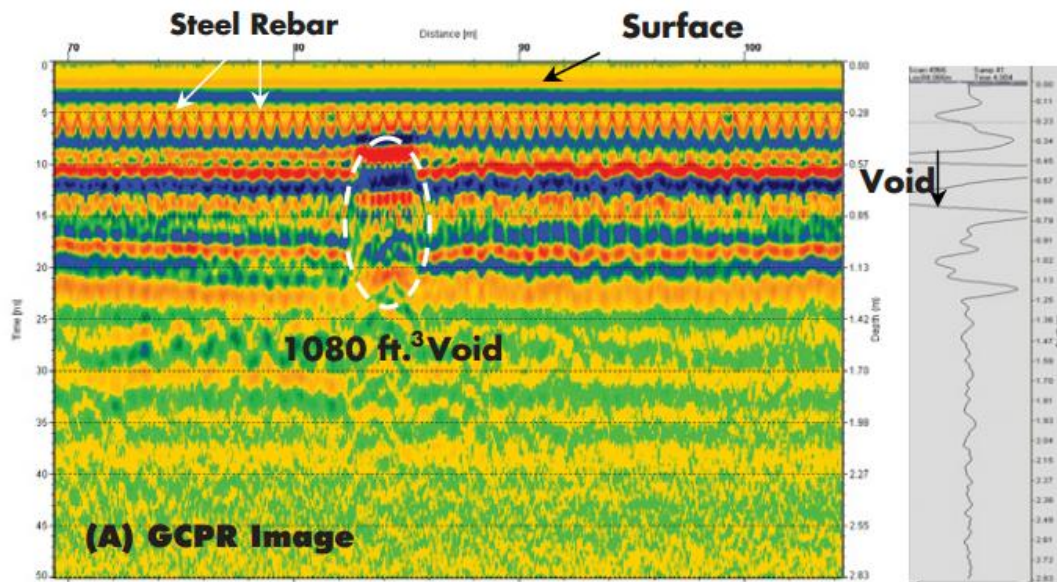

Figure 10. Radar Gram Results for U.S. 290 near Austin, T.X. (Chen, 2010).

Chen outlines an additional case study in Amarillo, Texas, concerning Interstate 40 (I-40). Similarly, a storm drain pipe had failed and soil fines were observed seeping out of the asphalt surface. After using GPR to survey the area, anomalies were noted on the radar gram in Figure 11.
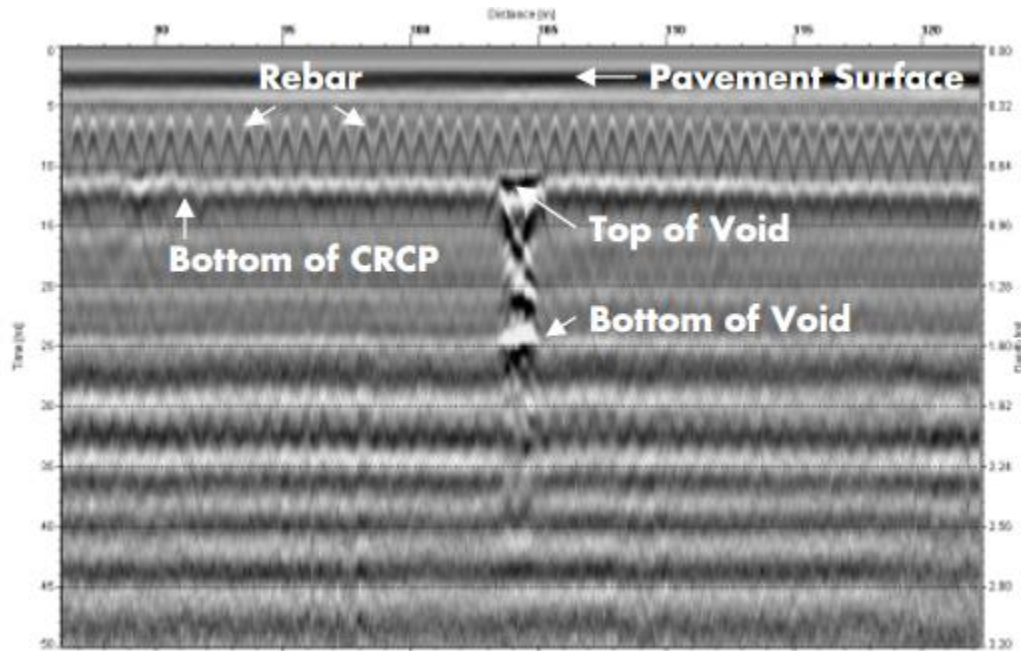
Figure 11. Anomalies from I-40 in Amarillo, Texas (Chen, 2010).

A section of the roadway was cut, and a 135 cubic foot void was realized (Chen, 2010). Figure 12 depicts the cut roadway, revealing a large void beneath the roadway surface. Remediation included grouting the void space.
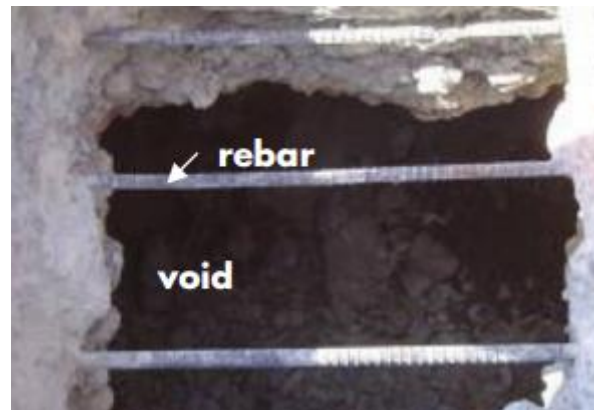

Figure 12. Void beneath I-40 detected by GPR (Chen, 2010).

The case studies are proof that radar scanning devices have helped in locating voids and soil anomalies. Overall, an additional study including FutureScan is necessary to help contractors and engineers verify their work and designs, respectively. Furthermore, few papers have been written on the subject of post-construction evaluation of trenchless projects.

Objective of Work

Evaluation of soil voids and anomalies, that can be created from HDD construction, is currently a qualitative method rather than quantitative. The engineer or technician, interpreting the radar gram results, uses their discretion when it comes to anomaly sizes and material type. Interpretation of radar gram results can differ from person to person; therefore, there is no base standard for anomaly characterization. Based on CUES, Inc. and FutureScan analysis, the testing firm has developed a system that is quite quantative. Reliability of FutureScan results must be tested so that a quantitative standard can be developed for the future.

The objective of this study was to point out the pros and cons of GPR and FutureScan, respectively. Through reliability testing of the products, conclusions based on field applicability, were determined. Reliability must be established so that Geotechnical engineers can depend on such devices in the future. The idea of such a study was to improve HDD construction by eliminating "black box" experiences, thus creating a means of assuring contractors and engineers that infrastructure has not been damaged.

Ultimately, a comparison of void or anomaly detection methods (GPR versus FutureScan) was made based on the results of scans in which target voids were installed prior to non-destructive radar testing. The installed target voids, made of foam, were comprised of various widths and thicknesses in an effort to establish degrees of accuracy. This study is unique, and a field comparison using this technology has not been established to date.

The various radar techniques were compared on three (3) separate project sites. Each test site entailed different pipes, pipe sizes, and depths of cover. Soil conditions from site to site are also noted. With varying test site conditions, the pros and cons of each machine were stated. A comparison of void or anomaly detection methods was made based on final results: GPR versus FutureScan. The pros and cons of each radar method were evaluated, relative to the three sites, along with a study of limitations. Also, the advantages and disadvantages of measuring origins (within pipe vs. on top of pipe) were identified.

To establish control for the experiment, target voids were installed prior to non-destructive radar testing at the Burnt Chimney project site. A series of target voids, made of foam, were installed throughout the test run. The goal was to evaluate the degree of accuracy of each machine.

In addition to the examination of the scan results, a correlation was derived between relative elevations and radar results for the Burnt Chimney project site. Surveyed elevations were logged before, during, after, and long after reaming the borehole. Radar results were recorded after pipe installation; therefore, a correlation between annular void space and the relative elevation could be attempted. A certain amount of annular space, detected shortly after construction, indicated a certain amount of settlement in the long-term. Also, a secondary correlation could be attempted between amount of upheave, annular space, and settlement in the long-term.

METHODS

Overview

Three (3) project sites are used for this investigation. The three sites will provide insight regarding pros, cons, and limitations that pertain to FutureScan and GPR. Each site will be described in the following paragraphs.

Burnt Chimney is considered the primary project site. The HDD project took place at Burnt Chimney. Burnt Chimney is located in Virginia, southeast of Roanoke. The Burnt Chimney project site is where reliability testing takes place using foam targets. The reliability of FutureScan is tested in this project site because target anomalies are capable of being installed, unlike the other two sites. Also, the Burnt Chimney site is crucial in correlating settlement/upheaval with FutureScan results. GPR will yield interesting at the primary site, for the drilled depths are rather deep. The measuring origin for FutureScan (i.e. pipe) could prove the advantage of using FutureScan in such a situation.

The following two sites are located along VA-635, southwest of Batesville, VA. The differences in the VA-635 sites are geographical location and pipe diameter. Polyethylene piping runs perpendicular beneath the roadway in both instances. The utilities were installed using the open-cut method, and reports indicate that backfill was not compacted properly. The piping is rather shallow at these locations and has been previously installed. So, no control is defined at the VA-635 sites. It is expected that GPR will be the prevailing method of anomaly location at this site due to measuring origin (i.e. roadway surface). This project site is used to make a better comparison of GPR to FutureScan, for compaction issues are apparently present throughout the soil cover above the utility.

Physical differences in the project sites are stated in Table 1. The differences in piping size and material allow for alternate test conditions. The difference in soil conditions and soil cover allow for GPR and FutureScan evaluation in completely different scenarios.

Table 1. Test Site Conditions.

Project Site	Pipe Size (in)	Depth of Cover (feet)	Pipe Material	Pipe Origin	Soil Conditions
Burnt Chimney	18	Varies from 5.0 to 8.0	HDPE	HD Supply	Virginia Piedmont (Dirty SANDS)
VA-635 I.	48, triple-wall	2.0	Polypropylene	ADS (Advanced Drainage Systems)	FILL – Crusher Run
VA-635 II.	30, double-wall	2.5	Polypropylene	ADS (Advanced Drainage Systems)	FILL – Crusher Run

Burnt Chimney Project and Site Soil Description

On October 30 of 2013, Grindstaff Underground, a directional drilling contractor, installed an 18-inch casing for a 12-inch water line for The Western Virginia Water Authority at the intersection of VA-116 (Jubal Early Highway) and VA-122 (Booker T. Washington Highway) in Burnt Chimney, VA. The test site was a relatively flat, developed region with existing elevations at approximately 1127-feet. The utility was drilled beneath VA-116. (See the outlined drill path overlain by ortho-imagery in Figure 12). One hundred and ninety (190) feet were drilled horizontally beneath existing grades. The HDPE (High Density Polyethylene) 18-inch casing, manufactured by HD Supply, was installed using horizontal directional drilling (HDD) methods. The GPS location (37.104,-79.816) reveals site soils are classified under the map unit symbol, 7C (USDA, 2013). Refer to the outlined drill path overlain by ortho-imagery (Figure 13A), and USDA established Web Soil Surveys relative to the drill path (Figure 13B).
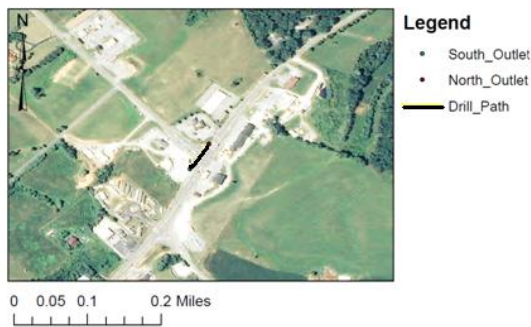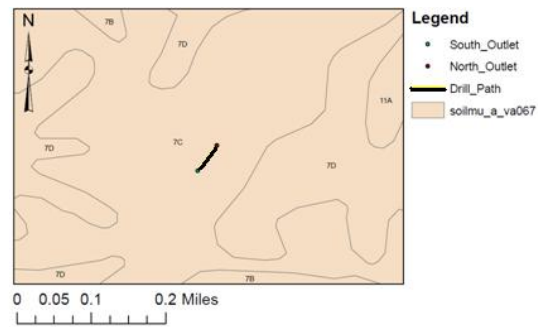
Figure 13A.   **Figure 13B.**

The map unit symbol defines a set of soil conditions with depth. So, map unit symbol, 7C, is defined by four soil strata down to 6.8-feet. Therefore, varying vertical strata were encountered during drilling. Table 2 is a boring log, describing 7C soils in the VA 067 soil region.

Table 2. USDA Soil Boring Log for Burnt Chimney Site (USDA, 2013).

Depth (feet)	USCS Classification	Fragments > 10-in (Percent)	Fragments >3-in (Percent)	Percent Passing: # 4 Sieve	# 10 Sieve	#40 Sieve	#200 Sieve	Liquid Limit (Percent)	Plasticity Index
0-0.60	SM, SC-SM	0	0-9	83-100	82-100	72-98	32-49	13-20	2-6
0.60-4.50	CL	0	0-9	81-100	80-100	72-100	60-100	31-45	13-31

4.50-5.2	SC-SM, ML, SM, CL, SC, CL-ML	0	0-9	81-100	80-100	57-100	40-80	13-34	2-14
5.2-6.8	CL-ML, SM, ML, CL, SC, SC-SM	0	0-9	81-100	80-100	67-100	37-76	13-34	2-14

The boring log in Table 2 includes particle-sizes, plastic limits, and USCS classifications. Table 2 gives a range of particle-size by mass that will be retained on U.S. sieve numbers: 4, 10, 40, and 200 for each outlined strata. Generally, finer-grained soils are seen at The Burnt Chimney site.

 In addition to the USDA boring log, laboratory tests were performed on soil cuttings from the project site. Results from ASTM D422, ASTM D4318, and D6913 procedures revealed that the average soil condition was that of a Silty-Clayey SAND. Refer to the soil laboratory testing section for the Burnt Chimney site.

Silty-Clayey Sands are primarily coarse-grained soils but also have large amounts of fine-grained materials. The primary fine-grained material in the soil composition is silt, which is cohesionless and non-plastic. Clay particles, which still exist in the soil makeup, account for approximately 22% of the total. Clay has high shrinkage/swell capability as well as high sensitivity to moisture additions. Therefore, the borehole drilled at Burnt Chimney is expected to have shrink or swell potential, despite its' high composition of sand and silt.

The Burnt Chimney site allowed for target voids to be placed around the utility's perimeter at the time of the site visit. Thus, deep void installation was made possible. The Burnt Chimney project was the primary site evaluated, and the specifications were pre-determined by The Western Virginia Water Authority. The Burnt Chimney project entailed HDD with HDPE pipe, unlike most jack-and-bore projects, which require ferrous pipes. FutureScan does not have the capability to send radar signals through metal or iron pipes, for dielectric constants of ferrous materials are infinite. So, successful results required non-ferrous piping systems. The project fit the pipe size requirements for the FutureScan technology (minimum 15-inch inner diameter), and the contractor gave researchers time to perform testing before pulling the inner casing through the 18-inch casing. FutureScan testing was held on the day after the HDPE casing was pulled through the borehole.

HDD Drilling Methods for Burnt Chimney Site

The average soil condition at the site was determined using a combination of data: USDA past history and ASTM laboratory soil investigation. Because varying strata were encountered during radar scanning, an average soil condition derivation was necessary. A 190 foot horizontally arc was drilled, and began at approximately 5 feet below grade on the north outlet and ended approximately 4 feet below grade on the south outlet, breaching a maximum depth of approximately 8-feet.

The contractor used a Vermeer D80x100 Navigator (Figure 14) directional drilling rig, which is capable of 20-degree pitches into the ground.

Figure 14. Vermeer Directional Rig (Photo by Frank Morris).

The 10-foot threaded rods allowed for bending at the connections. By changing pitch while drilling, a drill path could be manually altered. Thus, the path was capable of forming an arc shape within the ground, avoiding existing utilities and infrastructure.

The first step in the 18-inch HDPE casing installation entailed drilling a pilot hole, using a 6-inch diameter conic bit. Drilling was performed from the south end of the intersection, and advancements were made toward the north end. Two receiving pits were dug for ease of pumping cuttings. Figure 15 depicts the drilling rods traversing through the southern receiving pit, pitching beneath the existing roadway.
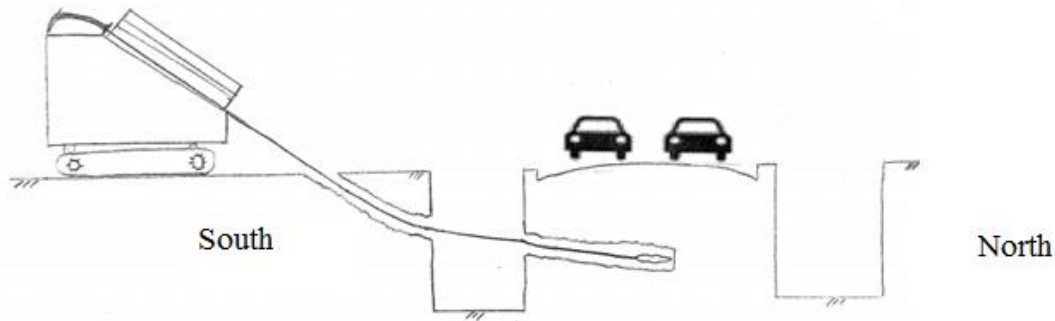
Figure 15. Drilling of the Pilot Hole beneath roadway.

Once the pilot hole reached the excavation on the north end of the intersection, the 6-inch bit was removed, and a large reamer bit was attached to the rods. The large ream bit was approximately 24-inch in diameter, and this bit was back-reamed through the pilot hole toward the south end. Bentonite slurry was pumped through the rod sections and out of the reaming bit. The bentonite slurry solution was mixed as such: 700-gallons of water to 100-pounds of dry powdered bentonite. As the rig turned the rods, the bentonite slurry was pumped through the weep holes in all directions, cutting the soil. This step of the drilling process followed the pilot hole back to the south end. The slurry and cuttings were pumped out of the excavation on the north end as drilling advanced.

Once the 24-inch diameter auger bit reached the south end, the rig pushed the bit back to the north end. The purpose of the additional drill was so that the casing could be pulled through the hole at the north end rather than being pushed from the south end. During pushing the bit back to the north end, slurry was pumped as needed. The additional pass through the drill path also further cleaned the hole.

Once the large auger bit reached the north end, the bit was removed, and a spindle was attached to the rod's end. Figure 16 displays the fitting plug on the end of the 18-inch HDPE casing attached to the spindle and kept the open casing from becoming filled with any soil. A closed-ended hook on the fitting plug allowed for shackle attachment at the drilling rod's end (Figure 17). After shackling the casing to the rods, the casing was pulled towards the rig from the north end to the south end, through the established drill path, thus completing the drilling.

Figure 16. Plug on end of 18-inch HDPE casing.

Figure 17. Spindle – Fitting Plug Connection.

Due to the reaming operations, a mixture of bentonite slurry and wet soil cuttings fills the annular space of the borehole. The 24-inch diameter auger bit leaves an approximate 24-inch inner diameter borehole for the HDPE casing. Because the casing has an 18-inch outer diameter, 3-inches of annular space is theoretically left all the way around the outer perimeter of the pipe. The mixture, bentonite and wet soil

cuttings, theoretically fills the annular 3-inch cut and is known as "filter cake." When the 18-inch casing is pulled through to the south end, "filter cake" seeps out into the receiving pit due to the volume loss of the open borehole. Many HDD projects include grouting the annular space as part of project specifications. Often, the annular space is simply left alone, and the "filter cake" is left to dry and harden with time. It is expected that the "filter cake" will dry and create a similar barrier as undisturbed soil. However, that may or may not be the case in the field.

Anomaly Targets for Burnt Chimney Site

To establish control and evaluate the reliability of FutureScan and GPR, target anomalies were installed prior to pipe inspection at The Burnt Chimney project site. The target anomalies were made of polyethylene foam wrapping. Manufactured in $1/16^{th}$ of an inch thickness, the wraps were cut and rolled around the pipe accordingly. The foam wrapping was then covered lightly with duct tape. Targets were installed along a non-critical section of pipe, meaning no foam wrapping was placed beneath the roadway or existing infrastructure. Refer to Table 3 for sizes and locations of targets. Figure 18 shows the pipe during insertion, displaying targets 2,3, and 4.

Table 3. Target Locations and Sizes.

Target	Distance from N. end of pipe	Spacing	Target Length (in.)	Target Thickness (in.)
1	37'-38'	2' (to joint)	12	¼
2	27'-27.5'	9.5' (1→2)	6	¼
3	25.5'-26'	1.0' (2→3)	6	¼
4	22.3'-22.65'	2'-11'' (3→4)	3	½

Figure 18: (Left → Right) White Marking, Target 4, Target 3, and Target 2. Target 1 not pictured.

Figure 19 is a depiction of the target region relative to the whole pipe. Note the pipe sections are 40-foot in length and were seam-welded at the joint locations. The seams are noted on the figure. Figure 20 is a "zoomed-in" view of the target location region, the last 40-foot section to be pulled beneath the ground.
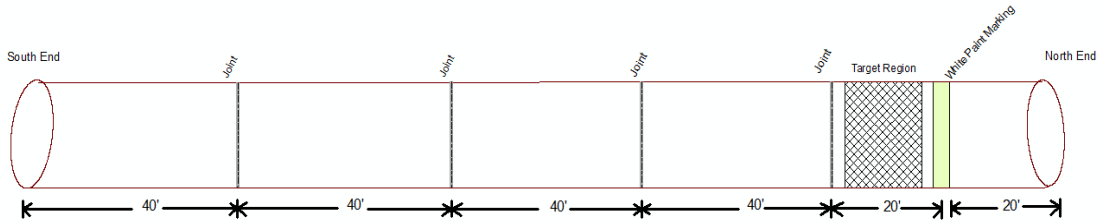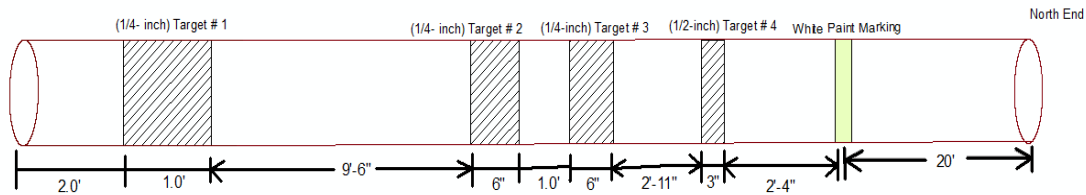

Figure 19. Target Region Relative to the Entire Length of Pipe.

Figure 20. Target Region "zoomed-in."

FutureScan

The target anomalies act as voids, for a change in dielectric constant indicates anomaly on the FutureScan radar screen. The target anomalies allow for three degrees of accuracy on account of FutureScan: spacing (location), target length, and target thickness. By establishing degrees of accuracy, FutureScan reliability can be determined.

Figure 21. FutureScan Robot (Photo by Frank Morris).

Two methods of non-destructive testing were used to find the pre-inserted voids at the site: Futurescan and GPR. Developed by Louisiana Tech University, FutureScan is now operated by an in-situ testing firm named CUES, Inc. FutureScan is a robot that can be sent directly inside the utility. Figure 21 shows a side-view of the FutureScan technology. Wheels are mechanically powered, and a coaxial cable attaches to the radar scanning device so that results are relayed through the coaxial cable during pipe entry. (See Figure 22.)

Figure 22. FutureScan Robot being inserted into Utility at Burnt Chimney Site (Photo by Lindsay Ivey Burden).

The technology can perform radar scans at 30-feet per minute along with camera frontal view. Coupled with a coaxial cable, FutureScan radar signals are transmitted simultaneously back to the source. Signal processing algorithms, setup by CUES, Inc., run in real-time as the robot advances further into the utility. The radar scanning antenna sits in front of the machine and receives reflections based on dielectric constant. Any change in dielectric constant will reflect a change on the radar gram; this would be considered an anomaly. The antenna can be shifted at various angles to complete a 360-degree rotation so that all of the utility can be inspected. Therefore, anomalies can be detected around the entire outer perimeter of the utility. Six equally spaced antenna shifts, also known as clock angles, allows for full antenna rotation: 12 O'clock, 2 O'clock, 4 O'clock, 6 O'clock, 8 O'clock, and 10 O'clock. Note that a new run must be performed for each new clock angle. Thus, six (6) runs were performed on site. Figure 23 displays the camera frontal view during advancement and the various clock angles.
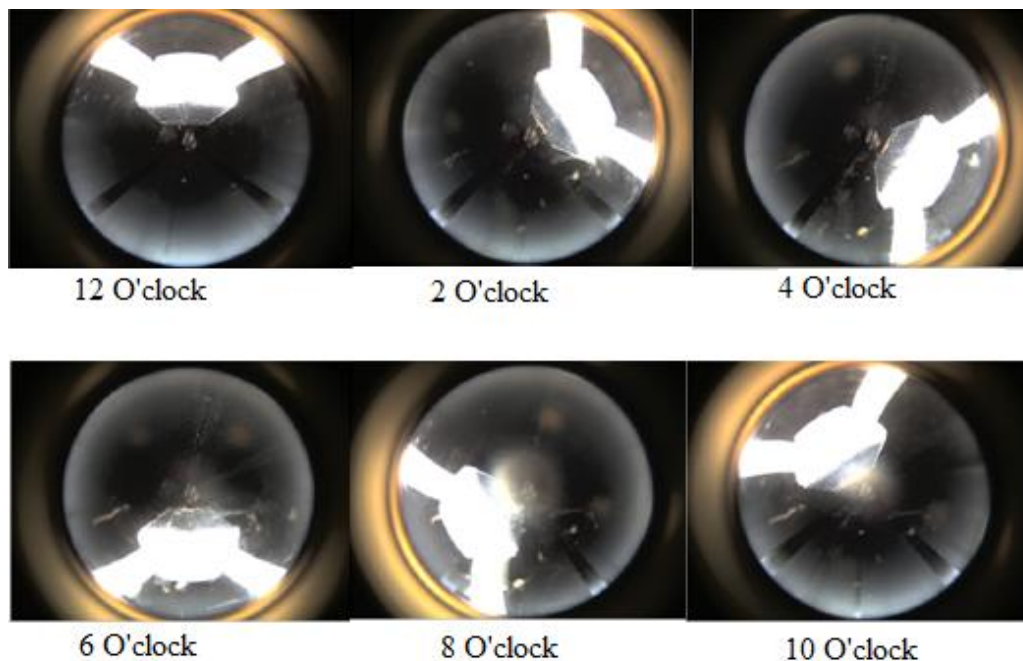
Figure 23. Various Clock Angles of FutureScan, Viewed from FutureScan Camera (Yestrebsky & Winiewicz, 2013).

The FutureScan Antenna radiates at a 30-degree angle beam-width and uses ultra-wide band antenna frequencies, ranging from 800 Megahertz to 5 Gigahertz. Therefore, very narrow pulses are utilized. A-Scans (Oscilloscope view) and B-Scans (Cross-sectional radar frequency gram) are performed for each run. Signal variations in the Y-direction are A-scans, and B-scans are sequences of A-scans. 512 samples are acquired equally spaced at 27 picoseconds compile a single sample of the B-scan; therefore, each sample is an A-scan. The number of samples is the scale on the Y-axis. The compilation of 27 picosecond samples creates the full B-scan or radar gram. In the results section of this paper, the B-scan will be the focal point.

FutureScan has the capability to measure pipe wall thicknesses and to detect voids on the outer walls of pipe. However, due to the method of radar scanning used and the size of the device itself, FutureScan can only operate in non-ferrous pipes larger than 15-inches in inner diameter. This is the major limitation to FutureScan.

CUES, Inc. offers two tiers of data analysis depending upon the number of runs performed: 1st tier and 2nd tier. Tier one analysis consists of qualitative void detection and bedding information. The 1st tier analysis can be performed at the time of the site visit, and the results are prepared immediately after the runs. Tier two analysis consists of more in-depth void information such as precise measurements of anomalies and precise distances relative to the origin. Algorithms calculate exact distances of signal inversion so that accurate volumes may be calculated. A comprehensive report including likely composition of anomalies and outlined radar grams is furnished for 2nd tier analysis. A 2nd tier analysis was performed for the Burnt Chimney scans; the 2nd tier analysis applies to this study because targets anomalies are very thin, and reliability is to be determined. Note that CUES, Inc. did not know the locations of the targets prior to performing FutureScan runs.

Ground Penetrating Radar (GPR)

GPR is primarily used to locate subterranean utilities. Shallow anomalies can most likely be detected by this method. Figure 24 is a depiction of the GPR cart system used for the Burnt Chimney project.
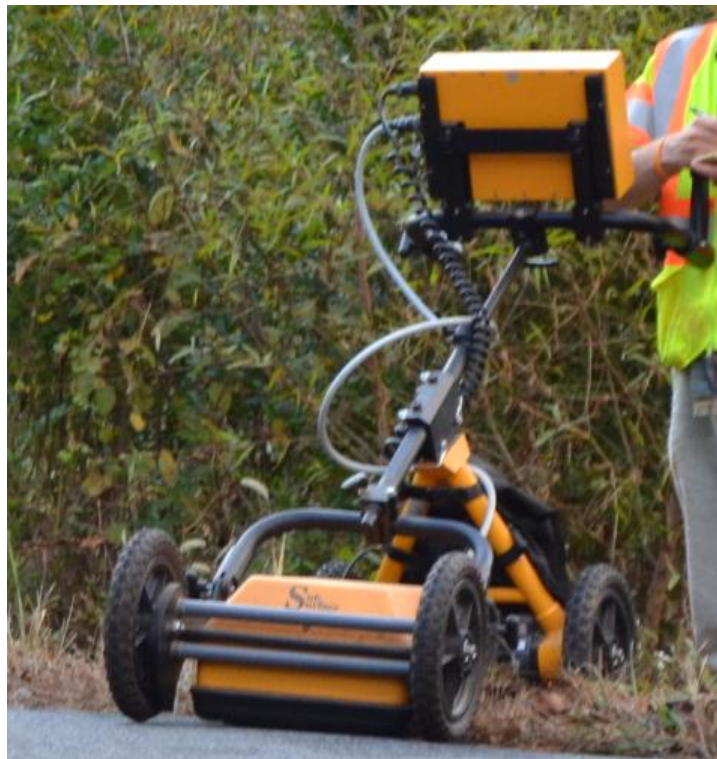

Figure 24. GPR Cart System (Photo by Lindsay Ivey Burden).

The GPR unit, used in this study, was made by USRADAR, Inc. The 500 Series Cart System rolls on the existing surface above the pipe and is capable of detection 15 feet below the surface, although the scale can be reduced down to 8.39 feet for improved accuracy. The radar scanning antenna sits flat on the front of a four-wheeled assembly. For this project site, the 8.39 foot scale was used. The antenna frequency range is between 300 and 1300 Megahertz, and the antenna pulse duration is typically 0.9 nanoseconds. The peak frequency is 500 Megahertz. The GPR unit uses Seeker SPR Acquisition software to display real-time results. Results are displayed in B-Scan Mode (Cross-sectional frequency gram mode).

Passes in the vicinity of the utilities on both sites are accomplished by simply pushing the cart system. Made at the asphalt surface, parallel and perpendicular passes are utilized at the VA-635 sites, where only parallel passes are made at the Burnt Chimney site due to safety constraints.

Laboratory Testing for the Burnt Chimney Site

A boring log was created from the Web Soil Survey in Burnt Chimney Project and Site Soil Description section. See Table 2 for the USDA boring log. Although this boring log was created, a representative soil sample was retrieved during reaming. The sample was transported back to the laboratory for further testing. Several samples of the cuttings and excavated material were made at intervals so that an average soil condition could be defined for drilling. Therefore, the total sample is indicative of the average condition in the field. Laboratory testing included Particle-Size using Sieve Analysis (ASTM D6913) and Hydrometer Analysis (ASTM D422). Plasticity was also determined by means of the Atterberg Limits testing (ASTM D4318). All ASTM standards and procedures were followed throughout experimental procedures.

A Hydrometer test in conjunction with Sieve Analysis was performed. An oven-dry amount of fifty (50) grams was used for this portion of testing.

First, a composite correction factor must be tabulated due to the Hydrometer reading being taken at the top of the meniscus. The 151H Hydrometer calibration by the manufacturer is performed at a constant temperature. Since the temperature of the liquid may not be the same as the manufacturer calibrated as well as temperature variances are likely to occur between readings, composite correction must be determined for a range. So, the composite correction takes into account reading differences from the zero reading for varying temperatures. A range of 16 degrees Celsius to 30 degrees Celsius is specified for Hydrometer testing, so the composite correction must be determined for every degree by linear interpolation from the minimum (16°C) to the maximum (30°C). The same solution used for testing must be used during composite correction factor determination. The solution consists of five (5) grams of granulated Sodium Hexa-metaphosphate with 1000 milliliters of deionized water. Hydrometer readings varied with temperature from the zero reading as shown below in Table 4.

Table 4. Composite Correction Factors for 151H Hydrometer.

Solution Temp (°C)	Composite Correction Factor, C
16	3
17	2.79
18	2.57
19	2.36
20	2.14
21	1.93
22	1.71
23	1.5
24	1.28
25	1.07
26	0.86
27	0.64
28	0.43
29	0.21
30	0

Laboratory results are displayed below in Table 5. Corrected Hydrometer readings are calculated by subtracting the composite correction factor from the actual Hydrometer reading. Note that the effective depth (L) is the effective depth of the Hydrometer in the soil mixture and is found from Table 2 of the ASTM standard. Also, note that K is a constant that depends on temperature of the mixture and specific gravity of the solids, which is found from Table 3 of the ASTM standard. A specific gravity of 2.70 is assumed for testing purposes; this value is indicative of fine-grained sandy soils. Example calculations of diameter of soil particles and percent of in suspension are shown below the table.

Table 5. Hydrometer Results.

Reading, T(min)	Hydrometer Reading, Actual	Effective Depth, L (cm)	Temperature (°C)	Composite Correction, C	Corrected Hydrometer Reading, R	Constant, K	Diameter, D (mm)	P (%)
2	1.016	12.1	24	1.29	1.0147	0.01282	0.0315	46.73
5	1.014	12.6	24	1.29	1.0127	0.01282	0.0204	40.37
15	1.012	13.1	24	1.29	1.0107	0.01282	0.0120	34.02
30	1.011	13.4	24	1.29	1.0097	0.01282	0.0086	30.84
60	1.0105	13.55	24	1.29	1.0092	0.01282	0.0061	29.26
250	1.0095	13.8	24	1.29	1.0082	0.01282	0.0030	26.08
1440	1.0075	14.3	23	1.5	1.0060	0.01297	0.0013	19.06

Particles in suspension (P) and Diameter of particle-size (D) are calculated using equations 1 and 5, respectively from the ASTM D422. Example calculations are shown below.

$$P = \left[\left(\frac{100{,}000}{W}\right)\left(\frac{G}{G-G_1}\right)\right] \cdot (R-G_1) = \left[\left(\frac{100{,}000}{50g}\right)\left(\frac{2.70}{2.70-1.0}\right)\right] \cdot (1.0147-1.0) = 46.73\%$$

$$D = K\sqrt{\frac{L}{T}} = 0.01282\sqrt{\frac{12.1cm}{2min}} = 0.0315mm$$

The parameter, G_1, is taken to be the specific gravity of the liquid in which the soil particles are suspended. G_1 is assumed to be unity for these calculations.

The Hydrometer test is the initial step in creating the grain-size distribution, for fines (silts and clays) are evaluated. The second step includes sieve analysis, which follows ASTM D6913. Results of sieve analysis include distributions of coarse-grained material (gravels and sands).

A nest of sieves stacked from largest to smallest opening is used for this test. The nest is shaken mechanically for the specified duration, and the amount of soil retained on each sieve is weighed in a cumulative manner. The results to the sieve analysis are below in Table 6.

Table 6. Sieve Analysis Results.

U.S. Sieve No.	Sieve Size (mm)	Amount Retained (g)	Percent Passing (%)
No. 4	4.75	0	100
No. 16	1.18	0.3	99.4
No. 30	0.6	1.2	97.6
No. 40	0.425	3.4	93.2
No. 50	0.3	8.2	83.6
No. 60	0.25	10.8	78.4
No. 100	0.15	19.1	61.8
No. 200	0.075	26.2	47.6

In combining the results from the sieve analysis and Hydrometer, Figure 25 is obtained. A full representation of the present grain sizes is displayed.
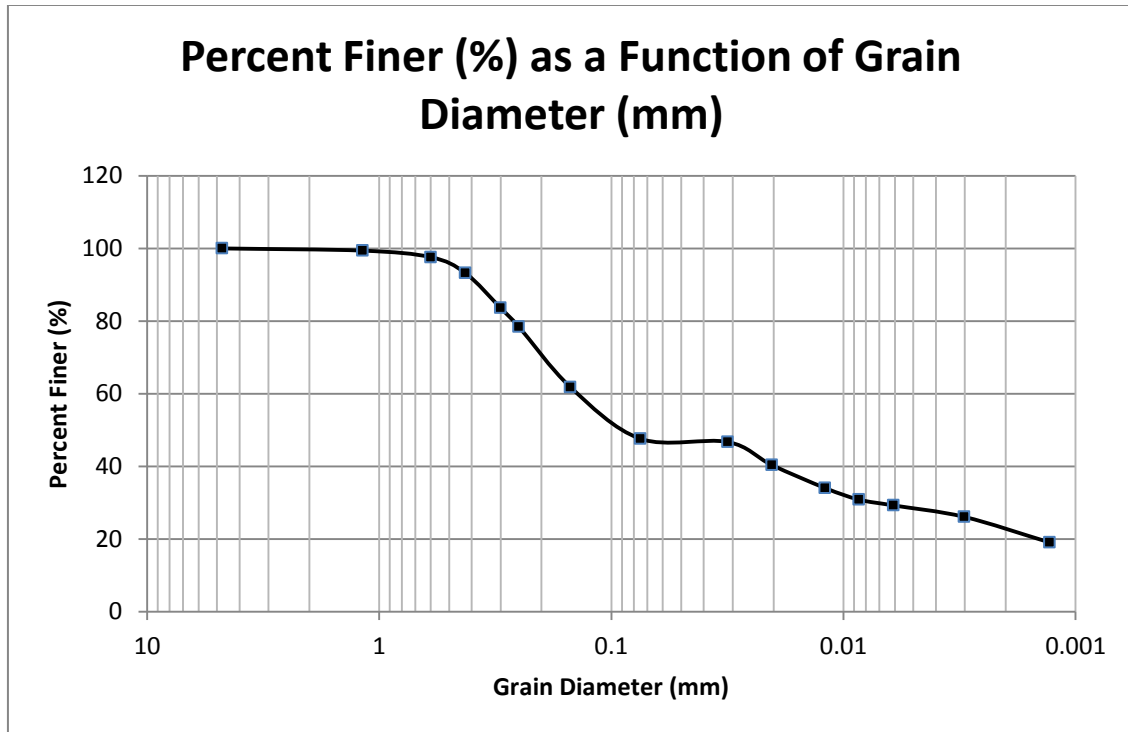
Figure 25. Grain-Size Distribution for Average Soil Condition.

Grain sizes for sands are considered by the USCS to be between 4.75-millimeters and 0.075- millimeters. From the above plot, 52.4% of the sample grain diameters are in the sand region. Thus, the sample is generally classified as sand. The next step in further classifying the sample is the Atterberg Limits test. Atterberg Limits further discern between silt and clay. Once a mortar and pestle was used to crush hard silts, the sample was ready to be sieved. After sieving the oven-dry material through the No. 40 sieve, the material was moisturized and prepared for the Atterberg Limits test. The results are shown below in Table 7. The moisture content as a function of blows plot displays the liquid limit of the soil in Figure 26.

Table 7. Atterberg Limits Test Results.

TARE No.	TEST	Blows	w (%)
23	PL	N/A	39.0
C-1	LL 1	30	52.6
29	LL 2	25	58.0
C-2	LL 3	20	62.7
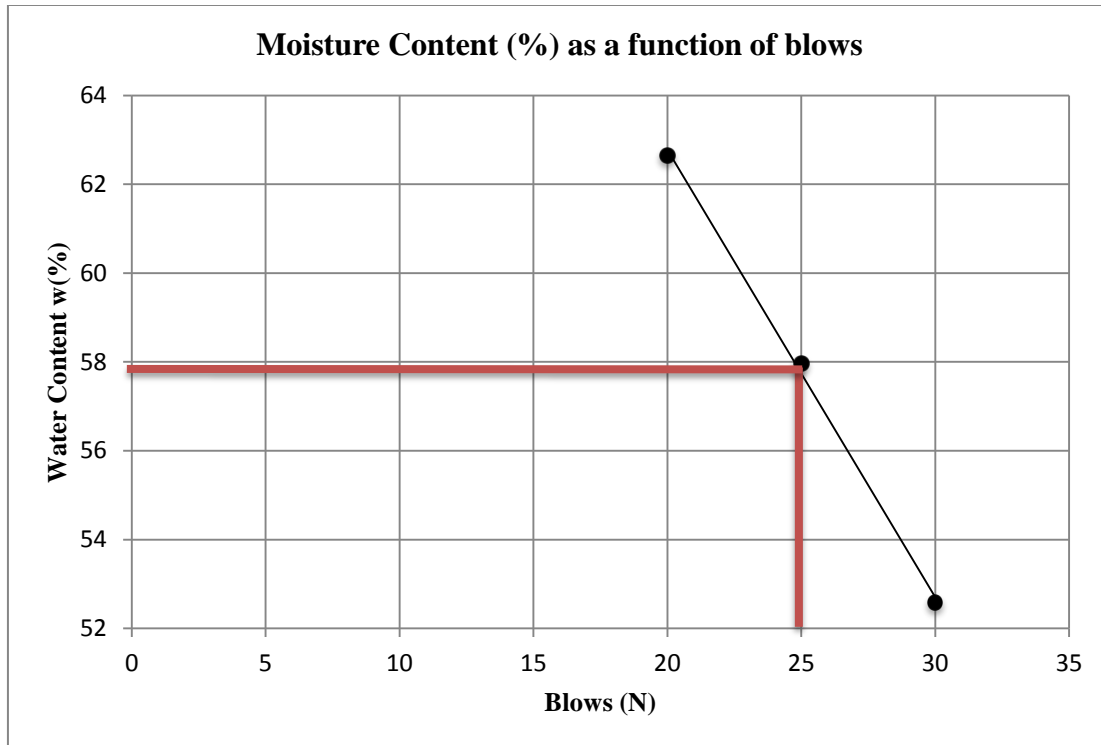
Figure 26. Atterberg Results plot.

The moisture content at 25 blows, liquid limit, in the Casagrande cup is seen at 58%. Note the red line at 25 blows in the plot above. The Plastic Limit subtracted from the Liquid Limit is known as the Plastic Index. From Casagrande's plasticity chart, the soil plots below the "A-Line;" therefore, the fines within the sample are classfied as primarily silty.

PL	39	%
LL	58	%
PI	19	%

Combining the results from the Grain-Size distribution and Atterberg Limits test, the Unified Soil Classification System considers the sample a <u>Silty-Clayey SAND</u>.

RESULTS/ DISCUSSIONS

Relative Elevations

Ten (10) relative elevations were logged across the entire roadway on approximate 15-foot centers. Figure 27 is a generalized depiction of the roadway and drill path during logging relative elevations.
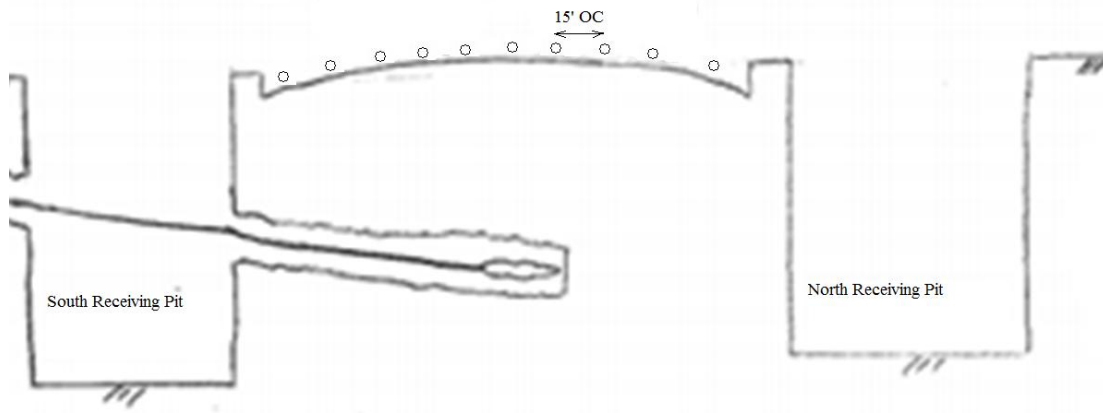
Figure 27. Cross-section of Roadway and Elevation Points.

Two different sets of elevations were logged during drilling: initial reaming toward the south end (during reaming 1) and pushing the auger through to the north end (during reaming 2). An average of the reaming elevation (during reaming 1 and during reaming 2) is tabulated to reduce any error that may have occurred during initial logging. The next set of elevations was recorded the day after reaming and pipe insertion. The final set of elevations was recorded four months after project completion.

Relative elevations are measured from Benchmark 1. Benchmark 1 is the top anchor bolt for a stop light pole on the south side of the intersection. The physical location of the elevations was marked on the asphalt in white spray paint so that the elevation recordings may be repeated. Figure 28 highlights road elevation points 2 and 3, facing in the northern direction.

Figure 28. Road Elevation Points 2 and 3 (Photo by Lindsay Ivey Burden).

A heaving trend was noticed during reaming. Two (2) sets of elevation data were recorded during reaming stages of the project. The average of the two sets of data is depicted below. Figure 29 is a cross-sectional view of the roadway during reaming, based on an exaggerated scale. The critical point, which appears approximately 150-feet from the north end of the pipe, experiences 1-inch of upheave. Heaves, ranging from 0.33-inches to 1.0-inch, are realized in Figure 29.
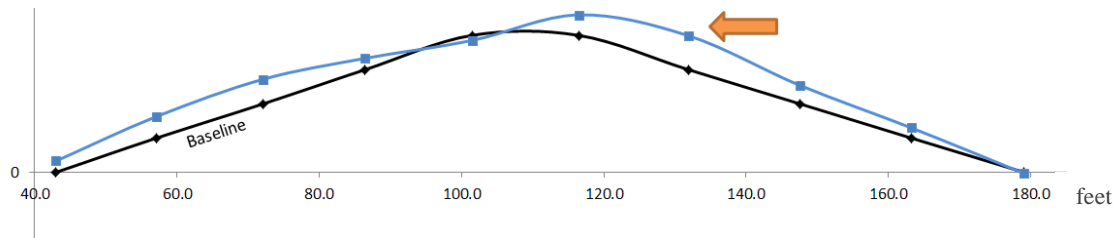
Figure 29. Roadway Movement during reaming.

The next figure displays the two actual sets of data recorded during reaming operations, relative to Benchmark 1. The baseline is also plotted on the same scale. One point in the crown of the road during the second round of reaming data seems to be especially low at 101.45-feet south of the north outlet of the pipe. The low point could be caused by surveying error. The basal upheave shown in Figure 30 is likely caused by drilling fluid pressures and the force of the reaming bit or by hydrofracture.
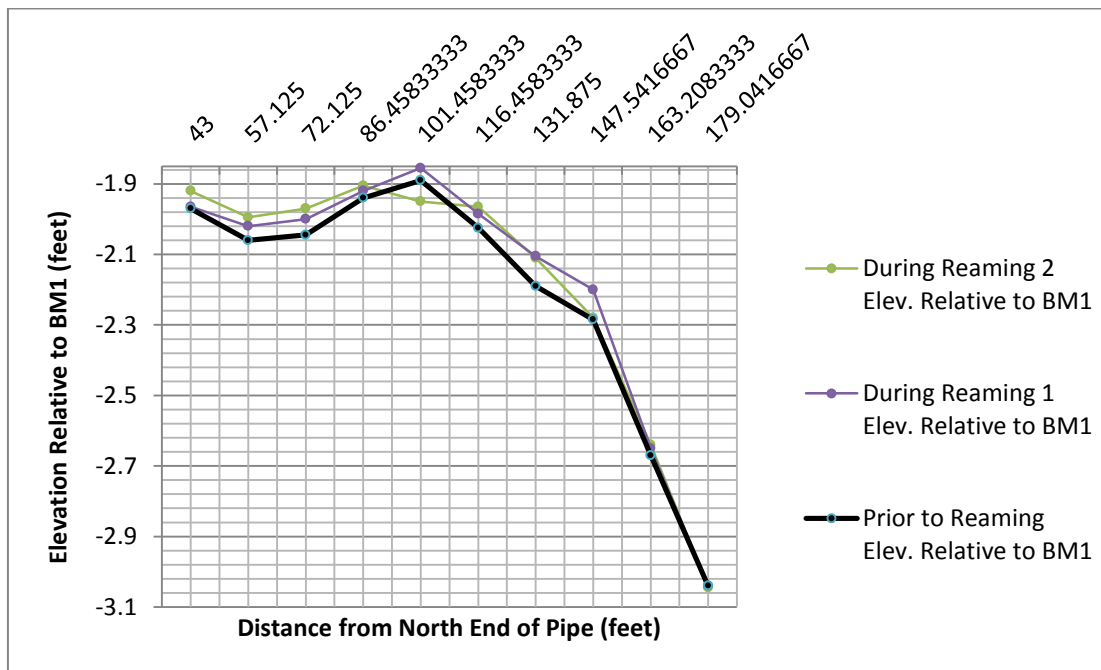
Figure 30. Relative Elevations during both reaming schemes.

Figure 31 displays the average of the two sets of reaming data versus the elevation data taken prior to drilling. Surveying error is minimized by averaging the sets of relative elevations. Notice that there still is a general upheave trend.
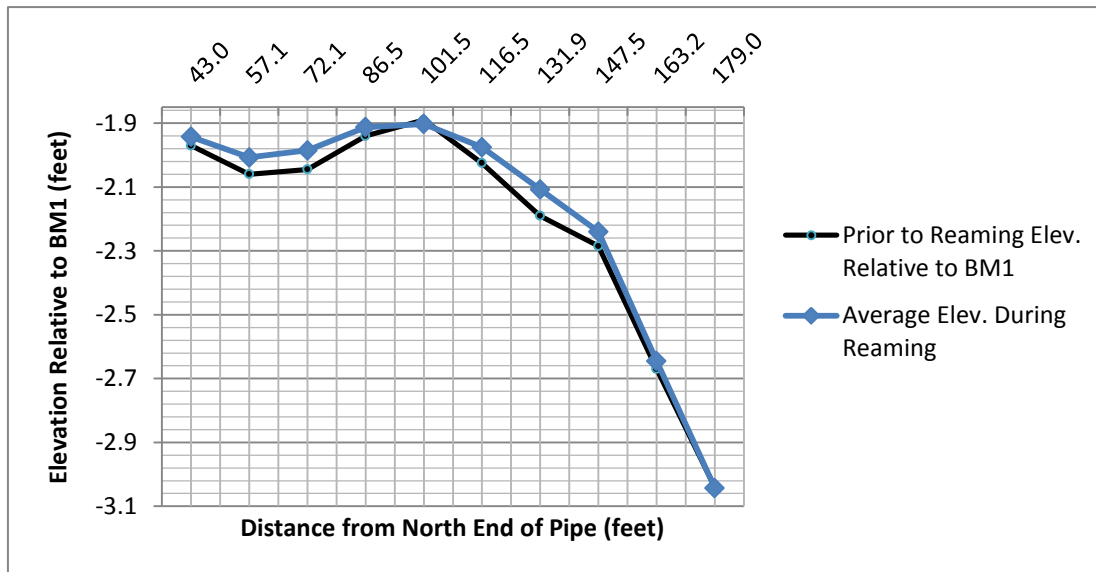
Figure 31. Average Reaming Schemes.

The drilling fluid pressures may have caused hydrofracture to occur within the soil above the pipe. Throughout reaming, heaving of the asphalt relative to the concrete gutter was noted. In Figure 32, approximately 3/4-inch of heave was noted between the south curb and concrete gutter.

Figure 32. Heaving of Asphalt relative to Curb and Gutter (Photo by Lindsay Ivey Burden).

While pushing the auger to the north end (During Reaming 2), drilling fluid started to come out of the edge of the asphalt on the south end (Figure 33). Moisture migrating from cracks or discontinuities in roadways is characteristic of hydrofracture. During hydrofracture, drilling fluid pressures exceed natural soil pressure of outer borehole walls, and cracks in the vertical direction begin forming. Fluid migrates through these cracks toward the ground surface. Drilling fluid comes to the surface to relieve hydrostatic pressures as shown in Figure 33.

Figure 33. Drilling Fluid migrating to the roadway surface (Photo by Frank Morris).

The relative elevations indicate hydrofracture occurred within this time frame. Basal upheave of the whole asphalt roadway was noticed. Signs of hydrofracture include both conditions: basal upheave and moisture release/cracking. Both indicators were seen on site.

The next set of elevations were logged on October 31st, 2013, the day after reaming and pulling the pipe, and plotted in Figure 34. Figure 34 is a cross-sectional view of the roadway the day after reaming, based on an exaggerated scale. The critical point, which appears approximately 90-feet from the north end of the pipe, experiences

0.90-inches of settlement. Settlements, ranging from 0.24-inches to 0.90-inches, are realized in Figure 34.
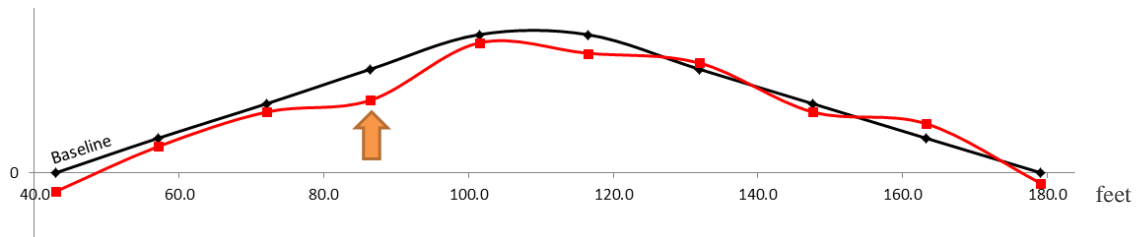
Figure 34. Roadway Movement after pipe insertion.

The actual elevation data is plotted in Figure 35, relative to Benchmark 1. A general settling trend is noticed in Figure 35. By this time, the borehole has had time to recede, and a slight amount of settlement occurred in the meantime. Potential weaknesses caused by hydrofracture and increased water content had likely caused the hole to recede. Note that October 31, 2013 was also the date in which FutureScan results were obtained.
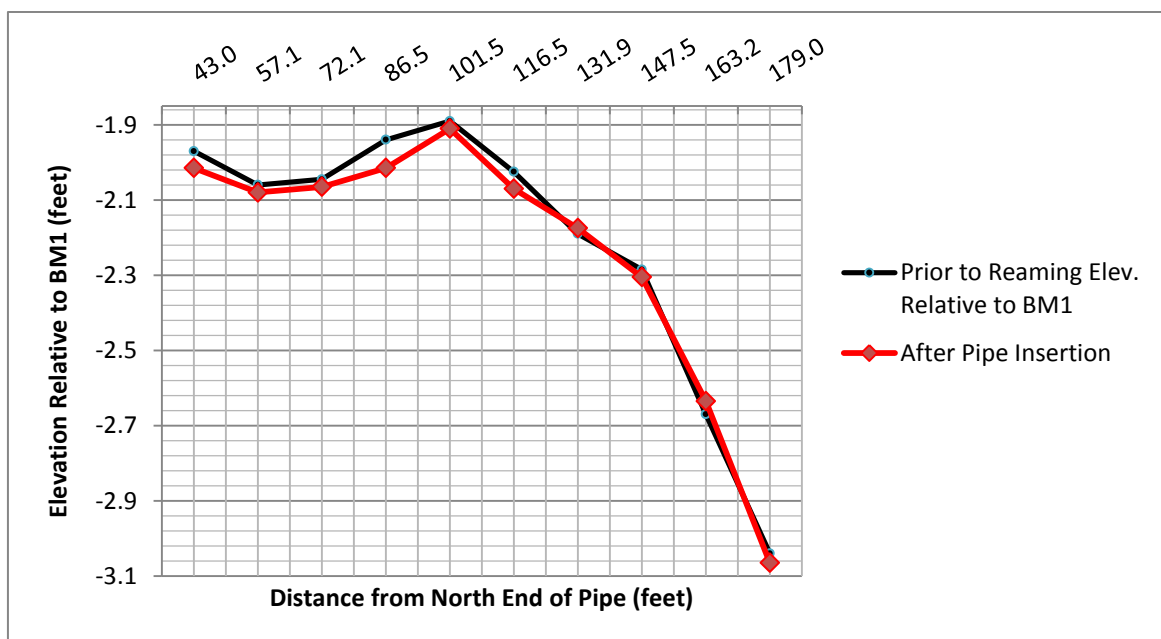
Figure 35. Elevations recorded the day after drilling operations.

A final set of elevations was logged four months after project completion so that long-term elevation results may be compared to FutureScan and GPR scans. Final elevation data was retrieved on site on March 2, 2014. Figure 36, an exaggerated cross-sectional view of the roadway, displays a heaving and settling trend: slight heave is shown on the ends of the pipe, and settlements are seen in the mid-section. The critical points, which appear at 115-feet and 165-feet from the north end of the pipe, experience 0.78-inches of settlement and 1.62-inches of heave, respectively. The range of settlements in the mid-section of the pipe is between 0.06-inches and

0.78-inches. The range of upheaves on the ends of the pipe is between 0.06-inches and 1.62-inches.
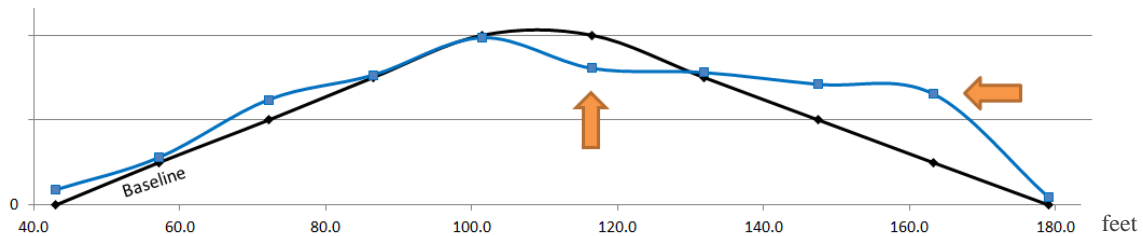
Figure 36. Roadway Movement four months after project completion.

Referring to Figure 37, heaving is noticed from 43-feet south of north end to 87-feet south of north end. Heaving is also noticed 132-feet south of north end to 179-feet south of north end. A settling trend is noticed in the middle: 101.5-feet to 132-feet south of north end.
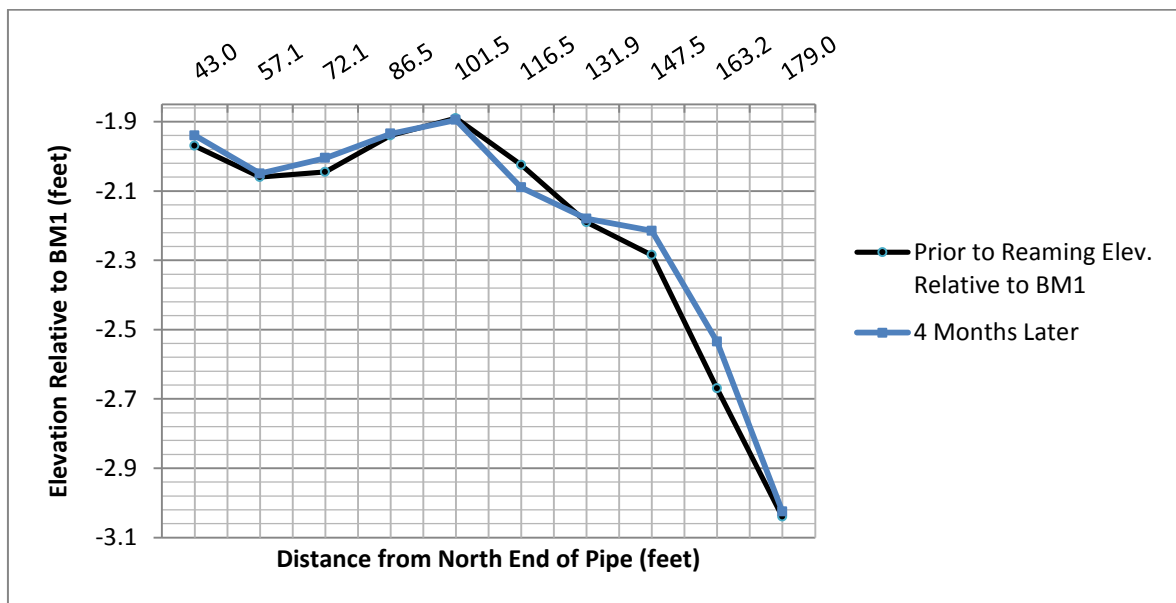

Figure 37. Elevations recorded 4-months after project completion.

FutureScan Results for Burnt Chimney

Five FutureScan runs were performed on site. Runs from the following clock angles were documented: 12 O'clock, 10 O'clock, 8 O'clock, 6 O'clock, and 2 O'clock. The various clock angles yield potential deficiencies that exist all the way around the outside of the pipe.

An anomalous region was detected by the FutureScan technology during the runs. Figures 38, 39, 40, 41, and 42 are B-scans from the 12 O'clock, 2 O'clock, 8 O'clock and 6 O'clock runs. Distance (feet) is on the X-axis, and the Y-axis is the sequence (frequency of samples) of A-scans. Note that the A-scan is considered the signal variation in the Y-direction. So, the B-scan is a compilation of 512 samples observed in the A-scan. Between 55-feet and 115-feet south of the north outlet, a large anamoly exists. Compared to the control (black line), many changes in dielectric constant occur on the radar gram. The region is detected in the middle of the piping section, where the signal variation is out of phase relative to the surrounding region.

From relative elevation data, this anomalous region also displayed heaving during drilling operations as well as settling shortly after drilling operations were complete. Heaving displayed uplifts between 0.33-inches and 0.72-inches in the noted anomalous region during drilling operations. The maximum heave recorded was 0.99-inches. Settlements, 24-hours after drilling, displayed subsidence between 0.24-inches and 0.90-inches within the anomalous region. The maximum settlement recorded was 0.90-inches. There is a strong correlation between the anomalous region and the upper surface (heaving and settling) during the construction period. In both cases, the maximum heave/settlement values exist in or near the anomalous region. Note the outer pipe wall (OPW) and inner pipe wall (IPW) designations on the below figures.

Figures 38, 39, and 42 suggest anomalies exist very close to the top outer pipe wall surface (See red outline in Figure 38). Note that these clock angles point in the direction of the ground surface; therefore, detected anomalies lie above the pipe. Anomalies detected above the pipe range from 1.3-inches to 4.6-inches in thickness. Figures 40 and 41 suggest anomalies exist further away from the outer pipe wall surface on the bottom half of the pipe, namely within the 1.5-inches to 4.5-inches. These anomalies exists below the pipe, for the clock angle points in the opposite direction of the surface. Overall, these results suggest that the casing is not centered in the open-cut. More void space is left below the pipe. Anomalies in both figures could be areas of void space or areas where the "filter cake" has thinned and annular overcut exists.
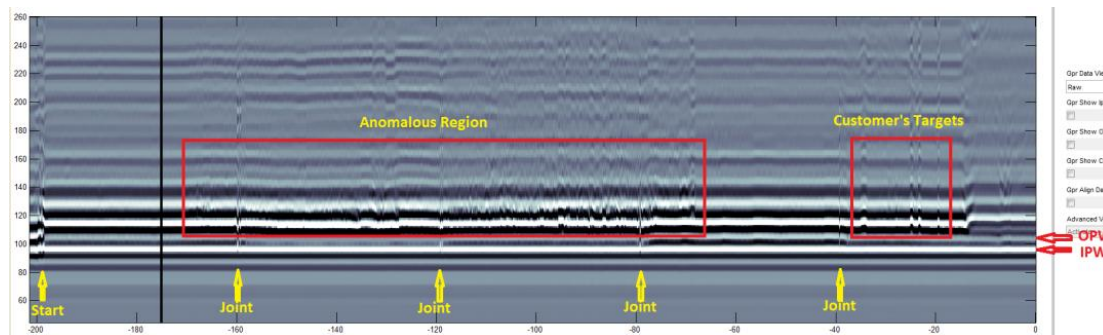

Figure 38. FutureScan Radar Gram at 12 O'clock position (Yestrebsky & Winiewicz, 2013).
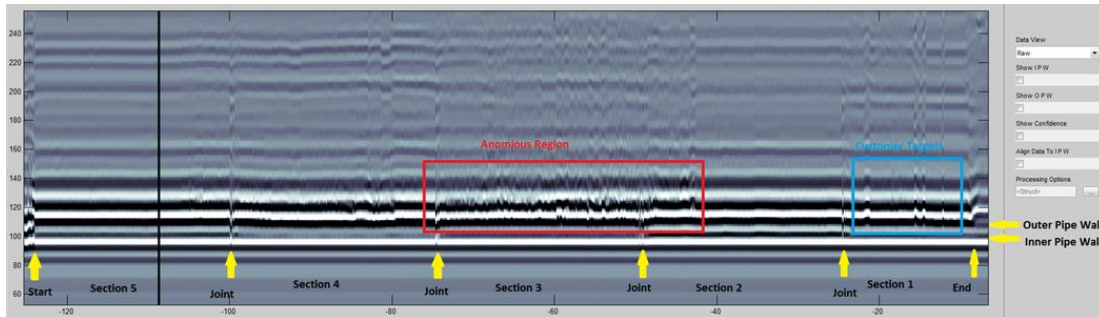
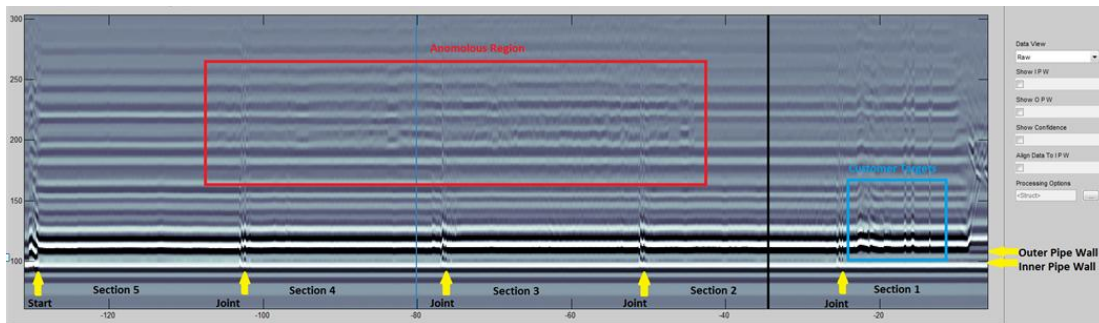**Figure 39. FutureScan Radar Gram at 2 O'clock position (Yestrebsky & Winiewicz, 2013).**

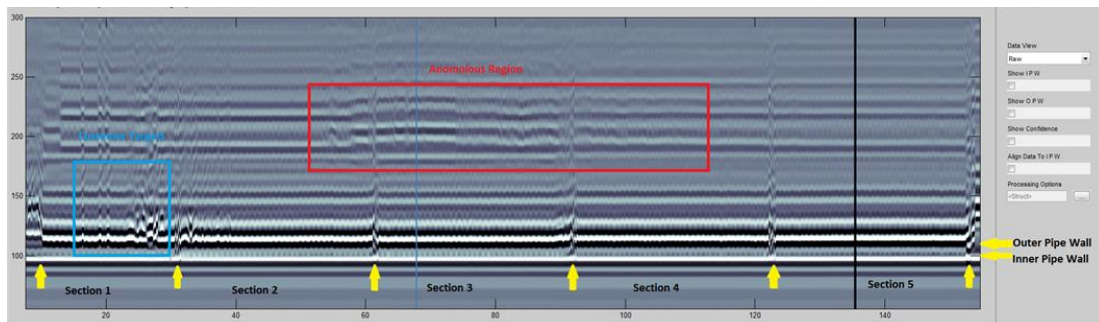**Figure 40. FutureScan Radar Gram at 8 O'clock position (Yestrebsky & Winiewicz, 2013).**

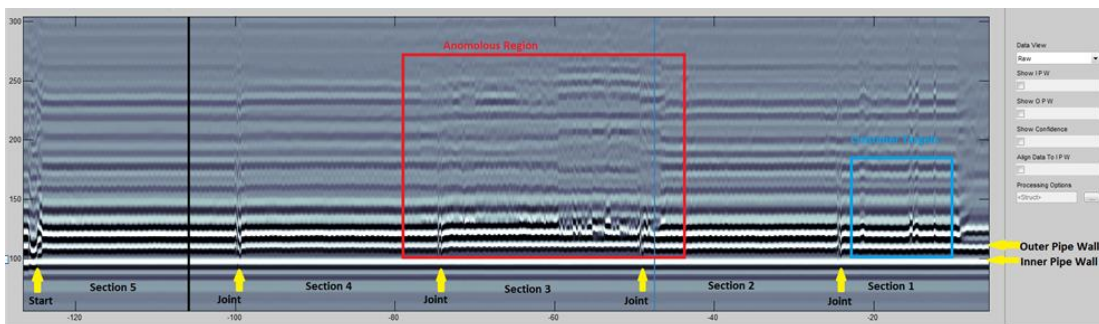**Figure 41. FutureScan Radar Gram at 6 O'clock position (Yestrebsky & Winiewicz, 2013).**

Figure 42. FutureScan Radar Gram at 10 O'clock position (Yestrebsky & Winiewicz, 2013).

Next, the scanning results at the time of the site visit (construction) are compared to the elevations recorded long after project completion. Four months after the project, an elevation transition is realized within the anomalous region seen in radar scans. Figure 43 is relative elevation data on the same scale as FutureScan radar scans. Settlements of up to 0.5-inches existing between 50 and 86-feet south of the north end. Heaving of the asphalt reaching approximately 0.80-inches exist, between 86 and 115-feet south of the north end. Beyond the detected anomalous region, 148-feet from the north end, a heave of 1.62-inches is observed. The detected anomalous region is subject to heaves and settlements after project completion. FutureScan defined a region, characterized by inversions of voltage, and large settlements and heaves were noted in a variety of scenarios.
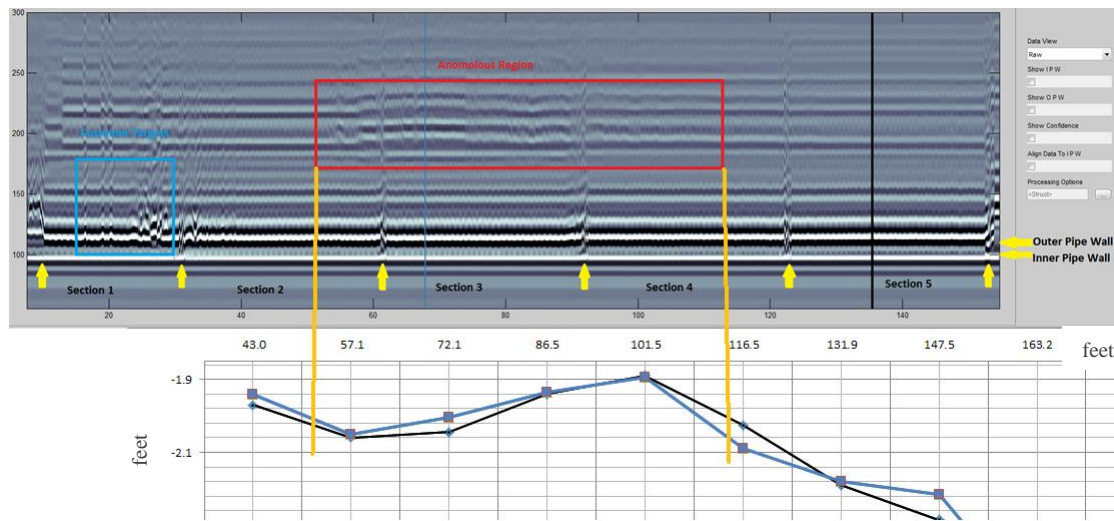

Figure 43. Elevation data relative to anomalous region (4-months after project completion).

An example calculation is necessary to illustrate conversion from Y-axis (Sequence of A-scans) to units of length. By using such a converison, distance to an anomaly may be tabulated as well as anomaly thickness. To illustrate the calculation, the 8 O'clock radar scan will be used as an example. The number of ticks on the Y-axis (27 picosecond samples of A-Scan) is counted from the outer pipe wall (OPW) to the beginning of the anomaly. In this case, 110 ticks are counted from the OPW to the bottom of the anomalous region (t = 110 units). Figure 44 displays the number of ticks from the outer pipe wall to the middle of the anomaly.
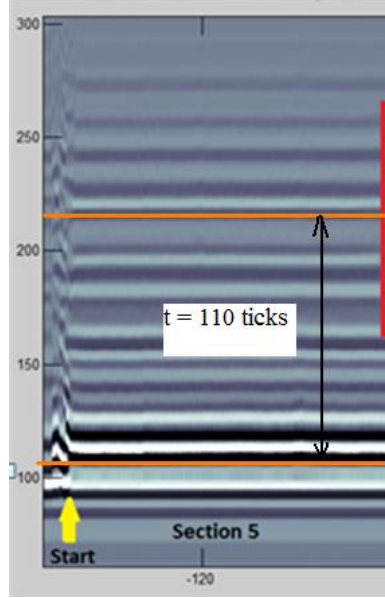
Figure 44. The number of ticks from OPW to the bottom of Anomalous Region.

The sampling rate is set at a constant 27 picoseconds. Therefore, A-Scan is extrapolated every 27 picoseconds to compile the total plot. The dielectric constant (k), of the silty-clayey sands at the Burnt Chimney site is taken to be an average of the given range, namely 30 (k = 30). The speed of light (c) is taken to be a constant $118x10^8\ inches/second$. The conversion from ticks to distance is calculated using the subsequent equation (Yestrebsky, Tom, Personal Communication, Febuary 25, 2014):

$$d = \frac{t \cdot T_s \cdot c}{2\sqrt{k}}.$$

From Figure 44, distance to the anomaly is tabulated:

$$d = \frac{(110\ units) \cdot (27x10^{-12}seconds/unit) \cdot (\frac{118x10^8 inches}{second})}{2\sqrt{30}} = 3.2\ inches$$

The middle of the anomaly exists at approximately 3-inches from the outer pipe wall, when scanning at the 8 O'clock position. This conversion is readily used to calculate thicknesses and distances of anomalies.

Table 8 lists anomaly distances from the OPW and thicknesses. Subsequent implications of roadway movement based on drilling procedure are listed in Table 9.

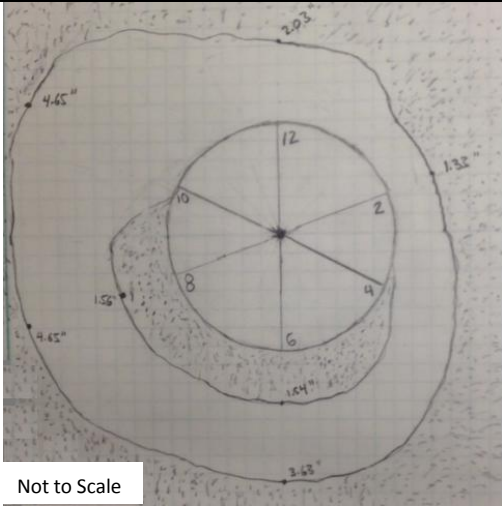**Table 8. Anomaly Locations and Thicknesses at Various Clock Angles.**

Clock Angle	Anomaly location from OPW (inches)	Anomaly Thickness (inches)	
10	0→4.65	4.65	
12	0→2.03	2.03	
2	0→1.33	1.33	
6	1.54→3.63	2.09	
8	1.56→4.65	3.09	

Not to Scale

Table 9. Construction Timeline and Implications.

During Reaming – Heaving (inches)	24-hours after Reaming – Settlements (inches)	4-months after Reaming – Varies (inches)
+0.30 to +0.99	-0.24 to -0.9	
+ 0.43 (average)	- 0.26 (average)	-0.78 to +1.62

GPR Results for Burnt Chimney

The entire width of roadway plus the northern grassed area beyond the curb (target region) was surveyed with the GPR rolling mount system. Starting from the south curb and heading toward the north outlet, 154-feet of subterrainain radar is shown below in Figure 45. The Y-axis displays depth in feet, and the X-axis displays distance in feet. The variation changes are shown in the figure relative to location (depth and distance travelled). GPR results are similar to the FutureScan B-scan plot in that inversions of voltage indicate anomalies on the radar scan.

Neither the 18-inch casing nor the targets were detected in the GPR results. The 18-inch HDPE casing traverses down to 8-feet within the surveyed region, and no changes in dielectric constant took place throughout the entire run below 4-feet on the radar gram. Other existing utilites were detected throughout the run. The parabolic pertubations on the radar gram indicate existing utilites perpendicular to the GPR pathway. The target foam wrap region was not detected during these runs either. This indicates that the GPR detection system cannot see below 4-feet accurately for this project site, or that once the GPR detects existing utilites, the technology cannot display any deeper pertubations. Depth of detection could be a function of soil type. This theory will be explored for the VA-635 sites.
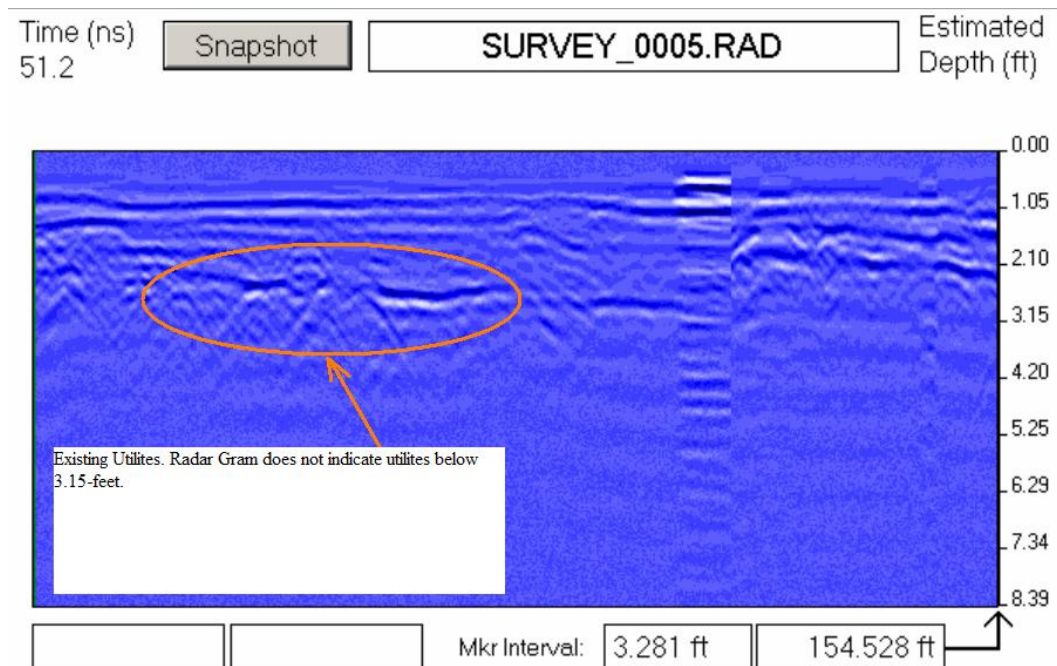
Figure 45. GPR radar gram.

FutureScan Results for Target Region

FutureScan was capable of detecting all target voids, while GPR was not capable of detection below 3.15-feet. Figure 46 is the FutureScan radar gram display for only the target region (20 to 40 feet from the north outlet). Similar to Figures 38, 39, 40, 41, and 42, the X-axis displays distance from the north outlet, and the Y-axis displays the sequence of variations of the A-scan. FutureScan was capable of detecting all target voids during the initial run. Lengths and thicknesses, similar to the ones installed, were detected on the scan. Note that the predicted length, thickness, and location was stated by CUES, Inc. on the scan itself.
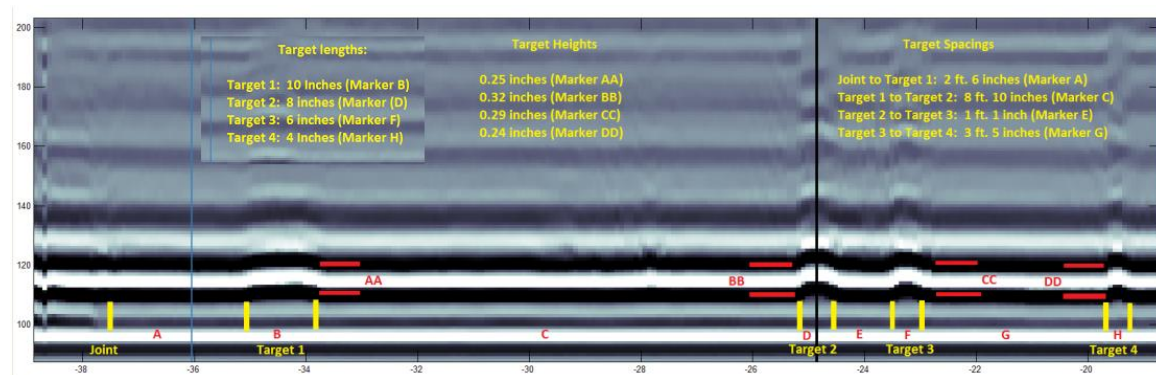

Figure 46. FutureScan radar gram "zoom-in" on Target Region (Yestrebsky & Winiewicz, 2013).

45

Although FutureScan was successful in detecting target anamolies, error did exist in the spacing of the final results. The reason for error in spacing was due to the measuring origin and the manual counting method. Because the manual counter was used, the wheel measurements did not align with the coaxial cable spool counter. The feed coming out of the spool was not aligned with the manual counter, which was directly relayed to the acquisition. Figure 47 highlights the spool and manual counter on the back of the CUES, Inc. truck mount.

Figure 47. The Manual Counter with Cable Feed (Photo by Frank Morris).

The reason for error in target length is due to the radar scanner being longer than the target it's measuring. If the targets were all greater than 12-inches, then the radar scanner could measure the targets to a more accurate degree. Due to the fact that all targets were under 12-inches and the scanner itself was 12-inches, it was difficult to accurately measure the target length. Table 10 shows the differences in the actual results and FutureScan results (See the highlighted columns). Table 11 calculates the error in spacing, target length, and target thickness.

Table 10. Comparsion with FutureScan results.

Target	Distance from N. end of pipe	Spacing	CUES Spacing	Target Length (in.)	CUES Target Length (in.)	Target Thickness (in.)	CUES Target Thickness (in.)
1	37'-38'	2' (to joint)	2'-6'' (to joint)	12	10	¼	¼
2	27'-27.5'	9.5' (1→2)	8'-10'' (1→2)	6	8	¼	.32
3	25.5'-26'	1.0' (2→3)	1'-1'' (2→3)	6	6	¼	.29
4	22.3'-22.65'	2'-11'' (3→4)	3'-5'' (3→4)	3	4	½	.24

Table 11. Error Calculations.

Target	Spacing Error (%)	Target Length Error (%)	Target Thickness Error (%)
1	20.00	16.67	0.00
2	7.55	25.00	21.88
3	7.69	0.00	13.79
4	14.63	25.00	52.00

The average spacing error for the four targets is 12.5%, the average target length error is 16.6%, and the average target thickness error is 21.9%. FutureScan is accurate to less than 6-inches in terms of length measurements. Also, FutureScan is accurate to 0.0925-inches on average in terms of thickness measurements. Overall, FutureScan is capable of measuring pertubations and anomalies within soil close to outer pipe walls. FutureScan will next be tested in opposition with GPR, where anomalies further away from the outer pipe wall exist.

VA-635 Project and Site Soil Description

In addition to the Burnt Chimney site, two (2) existing drainage pipes were also inspected via FutureScan and GPR. The two pipes are approximately 2-miles apart on VA-635. The first pipe was a 30-inch dual-wall polypropylene pipe, and the second pipe was a 48-inch dual-wall polypropylene pipe. The site location, site soils, and history are described below.

During July of 2009, Virginia Department of Transportation (VDOT) installed two (2) utility pipes at location along VA-635 in Albemarle County, southwest of Batesville (Figure 48). The exact location of the first pipe is north of Blackberry road on Route 635. Ortho-imagery for the GPS location (37.96555,-78.771375) is shown in Figure 48. The site elevation is approximately 745-feet; the site grade was filled

above natural grades for roadway purposes. The first pipe installed is a 30-foot section of 30-inch diameter dual-wall polypropylene piping (Hoppe, 2011). For this project, the open-cut trench method was used, excavating a 10-foot wide and 6-foot deep ditch (Hoppe, 2011). The utility currently spans perpendicularly beneath the VA-635 roadway. Bedding material consisted of No. 57 stone, and the backfill material consisted of No. 26 crusher run (Hoppe, 2011). During construction, backfill compaction did not take place, although surface compaction took place using a 4100 Gradall excavator (Hoppe, 2011). Since pipe backfill and bedding is composed of fill rather than natural deposits, a USDA derived boring log was not created for this project site.

Radar imaging was conducted at this site to provide insight regarding scanning capability within coarse-grained soils and poorly compacted regions. HDD practices were not used during construction, and the pipe embedment is shallow. GPR results should be able to pick up possible anomalies, considering the shallow pipe cover. FutureScan's results will be of interest because known areas of poorly compacted backfill exist close to the roadway surface. Results will provide insight as to the FutureScan's capability in measuring relative density of fills. FutureScan's scanning distance will also be tested due to the larger size of the pipe and anomaly distance from the scanner.
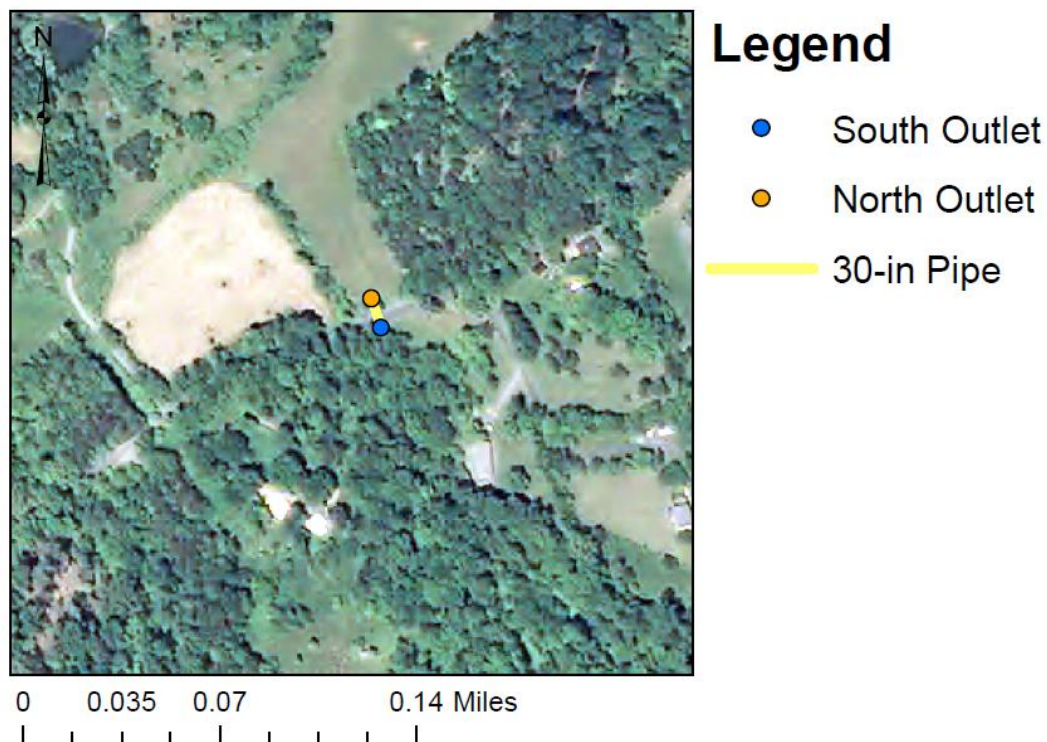

Figure 48. 30-inch Dual-Wall Polypropylene Pipe (PP) Overlain by Ortho-imagery (USGS, 2013).

The second pipe installed in July of 2009, along VA-635 is a 33.5-foot, 48-inch diameter triple-wall polypropylene piping section. The exact location of the pipe is

south of Kacey Lane on Route 635. Ortho-imagery for the GPS location (37.957531,-78.783659) is shown in Figure 49. The site elevation is approximately 700-feet; the site grade was filled above natural grades for roadway purposes. Again, the open-cut method was used across the roadway, excavating a 10-foot wide and 7-foot deep ditch (Hoppe, 2011). The utility now spans beneath the existing VA-635 roadway. Bedding material consisted of No. 57 stone, and the backfill material consisted of No. 26 crusher run (Hoppe, 2011). As with the 30-inch diameter pipe, backfill compaction did not take place, although surface compaction took place using a 4100 Gradall excavator (Hoppe, 2011). A boring log was not created from the Web Soil Survey (WSS), since the pipe backfill and bedding was composed of fill rather than natural deposits.
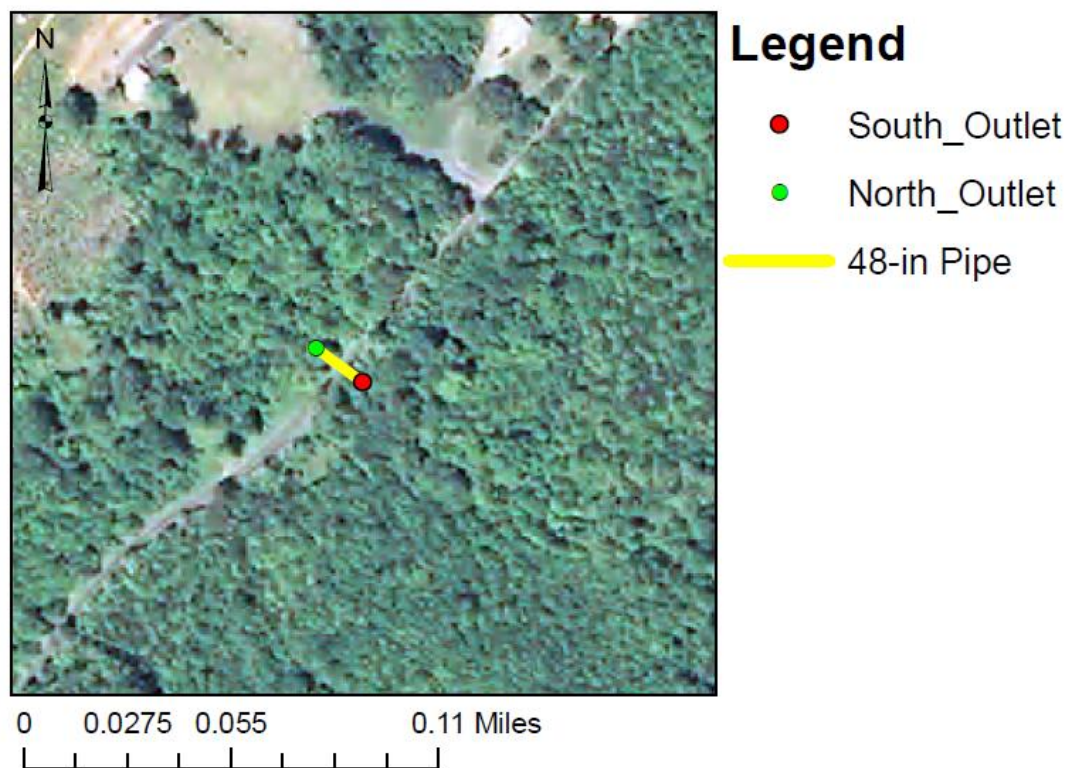

Figure 49. 48-inch Triple-Wall Polypropylene Pipe (PP) Overlain by Ortho-imagery (USGS, 2013).

The VA-635 sites were evaluated with GPR and FutureScan well after construction. With permission from the VDOT project manager and engineer, researchers performed in-situ radar testing on site.

GPR Results for VA-635

The various site conditions encountered in this study allowed for limitations of both radar technologies to be explored. Fortunately, the VA-635 piping systems were shallow enough for GPR detection, whereas the Burnt Chimney piping systems were not shallow enough for detection from the surface.

The GPR results for VA-635 are deemed sucessful in locating anomalies closer to the asphalt surface. GPR results for project site VA-635 are shown below in Figures 50 and 51. These figures are for the same runs performed on the triple-wall 48-inch polypropeleyne pipe. The first figure (Figure 50) outlines anomalies existing close to the outer pipe wall surface, whereas the second figure (Figure 51) outlines anomalies that lie close to the asphalt surface. In Figure 50, anomalies are detected above the pipe between 13-feet and 16.5-feet (downstream) north of the south outlet. The anomaly is quite large and within 1-inch from the outer pipe wall surface. The anomaly, in this case, is shown to be between 2 and 3-inches thick. Because compaction did not take place during construction, large voids or anomalies are expected. Also, punctures in the pipe were noted during construction in this region (Hoppe, 2011). So, a breach in the pipe wall is a possible defect.
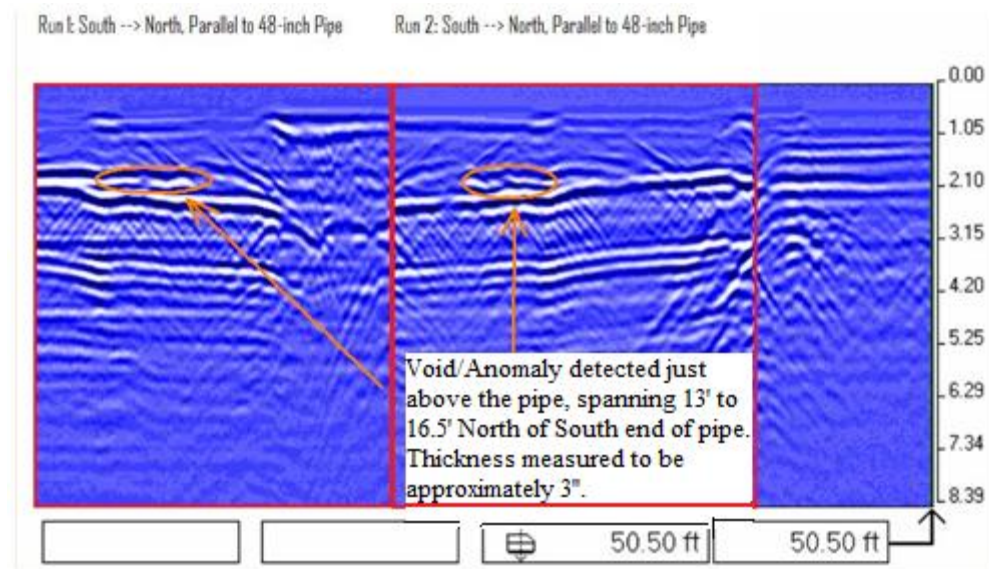

Figure 50. VA-635 48-inch Triple-Wall Polypropylene Pipe (PP).

Figure 50 is the essentially same as Figure 51, but a single anomaly closer to the surface is noted. Relative to other measurements on the radar gram, this anomaly seems to be 2 to 3-inches in thickness, spanning between 14'-4'' and 15'-3'' north of the south outlet of the pipe. The length of the anomaly spans approximately 8-inches. In this scenario, GPR is capable of measuring voids, anomalies, and disturbed soils close to the surface. The antenna is close to its' targets with no other interference and is capable of detection, unlike the Burnt Chimney project site conditions.
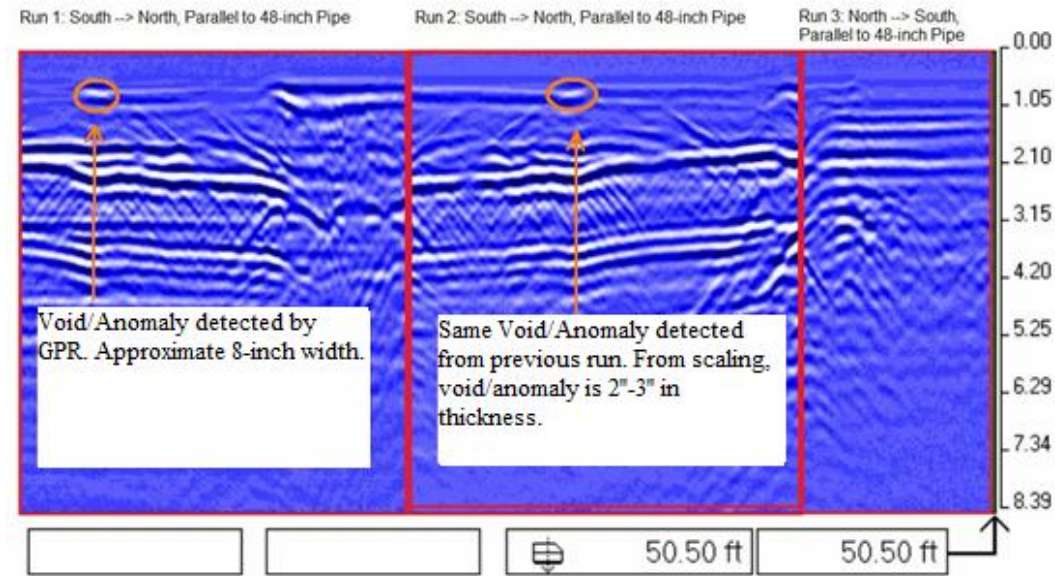
Figure 51. VA-635 48-inch Triple-Wall Polypropylene Pipe (PP).

GPR was tested making perpendicular passes at the existing 30-inch polypropylene pipe on VA-635. Perpendicular runs at the asphalt surface were made, and the GPR cart system was turned 180-degrees to make sequential passes a few feet beyond the utility. Inconsistent results were achieved when making parallel passes; results were not decipherable. An anomalous region is shown in Figure 52, existing approximately 8-inches above the outer wall. The length of the region spans 8-inches and is approximately 2-inches thick. The anomaly could be a homogenous spanning void or a seam of poorly compacted soil.
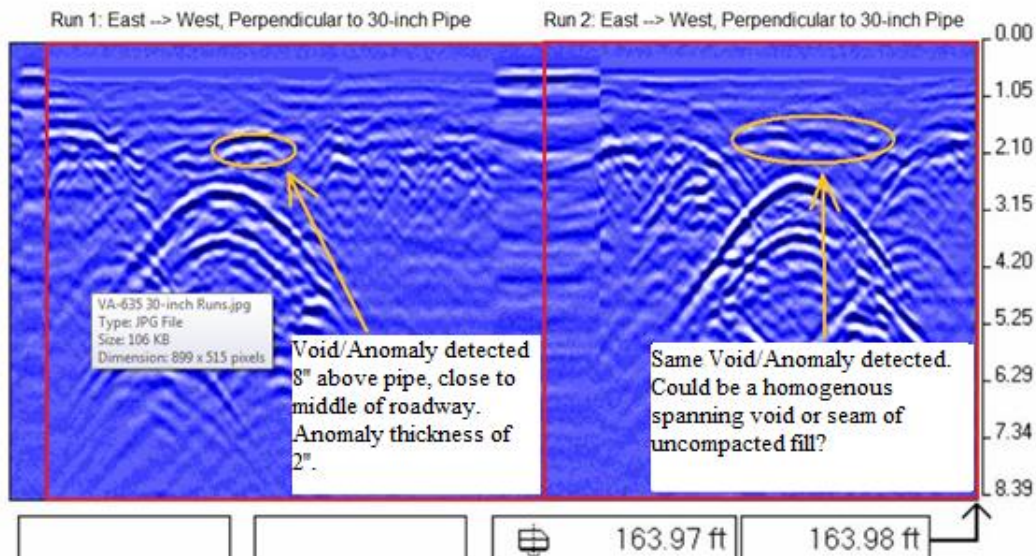
Figure 52. VA-635 30-inch Dual-Wall Polypropylene Pipe (PP).

In the case where there is not much soil cover on top of the pipe, GPR is capable of measuring soil anomalies above the pipe. Two (2) feet of soil cover exists on top of the 30-inch piping system, and GPR was capable of viewing this region for anomalies.

FutureScan Results for VA-635 sites

FutureScan results align with GPR results, pertaining to the anomaly near the 48-inch PE pipe wall. The anomaly at the outer pipe wall surface, between 13-feet and 16.5-feet downstream, was detected by GPR. FutureScan detects the anomaly at approximately 14-feet downstream in Figure 50. A well-defined breach in the pipe wall is noticed in FutureScan data, depicted in Figure 53. During the construction phase of the project, indentations were noticed by Virginia Department of Transportation engineers (Hoppe, 2011). Compaction issues closer to the asphalt surface were not detected by FutureScan. However, FutureScan and GPR results align, relative to the anomaly closer to the outer pipe wall surface.
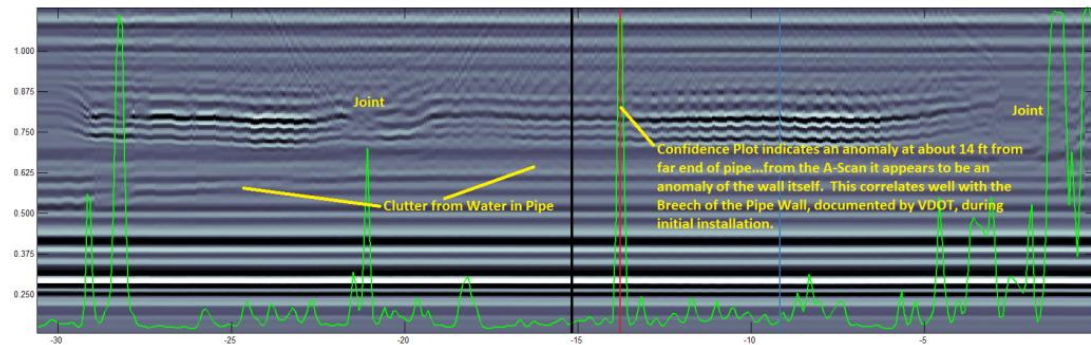

Figure 53. FutureScan Radar Gram at 12 O'clock position for VA-635 48-inch PP pipe (Yestrebsky & Winiewicz, 2014).

Because water was in the pipe during scanning, voltage inversions appeared misplaced on the radar gram. This is the reason that FutureScan could not detect compaction or void issues close to the asphalt surface. Cluttered inversions appeared closer to the asphalt surface due to the nature of the wet pipe. Expected signals would have been anomalies approximately 1-foot from the outer pipe wall as displayed in Figure 51.

Clutter terms result from backreflected signal due to surrounding environment (Nathanson, 1969 quoted in Grazzini, et al., 2007). Clutter can be a static or dead signal (Grazzini, et al., 2007). In this case, water, surrounding the bottom half of the scanning device, was causing static signals. As a result, anomalies were not detected near the asphalt surface. Therefore, no comparison is to be made based on the detected GPR near the asphalt surface.

Scanning signals tend to leak out of the back the antenna, and this causes a error signal (clutter) in the radar return (Yestrebsky, Tom, Personal Communication, April 9, 2014). With a constant water depth, the clutter signal can be subtracted on-site; however, water depth was not constant during data acquisition due to the pipe being backed up with water (Yestrebsky, Tom, Personal Communication, April 9, 2014). Clutter cancelling systems exist, but initial signals must be reduced immediately after acquistion. Digital phase shifters and attenuation must be utilized as an initial element to the signal receiving system to reduce undesirable signals (Grazzini, et al., 2007). GPR does not experience the signal leakage and back-reflection issue because leakage signals point in the direction of the sky.

FutureScan was unsuccessful in locating soil anomalies for the 30-inch PP pipe, for the same cluttering occurred during field trials. Water was readily flowing in the PP pipe during the testing period, so clutter inversions existed on the radar gram. Several inches of water existed in the pipe during the site visit. GPR detected an anomaly approximately 8-inches from the OPW surface, and FutureScan was incapable of detecting the same anomaly. Figure 54 displays the clutter terms that prevent anomaly detection, pertaining to the 30-inch piping system underneath VA-635
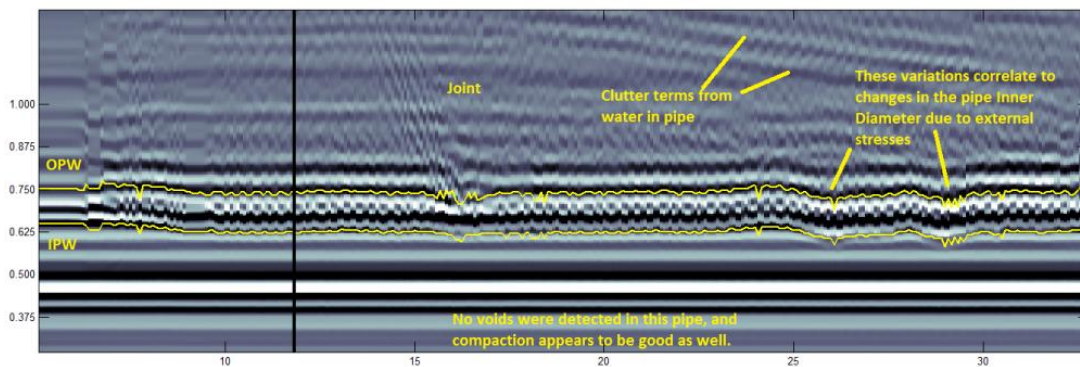

Figure 54. FutureScan Radar Gram at 12 O'clock position for VA-635 30-inch PP pipe (Yestrebsky & Winiewicz, 2014).

CONCLUSIONS AND RECOMMENDATIONS

Summary

FutureScan detected a large anomaly system near the midpoint of the pipe at the Burnt Chimney site. On the asphalt surface, this region experienced a significant amount of movement. An average of 0.43-inches of basal upheave was noticed during drilling operations, whereas an average of 0.26-inches of settlement was noted one day after drilling operations came to an end. In both phases of construction, the roadway saw approximately 1-inch of movement.
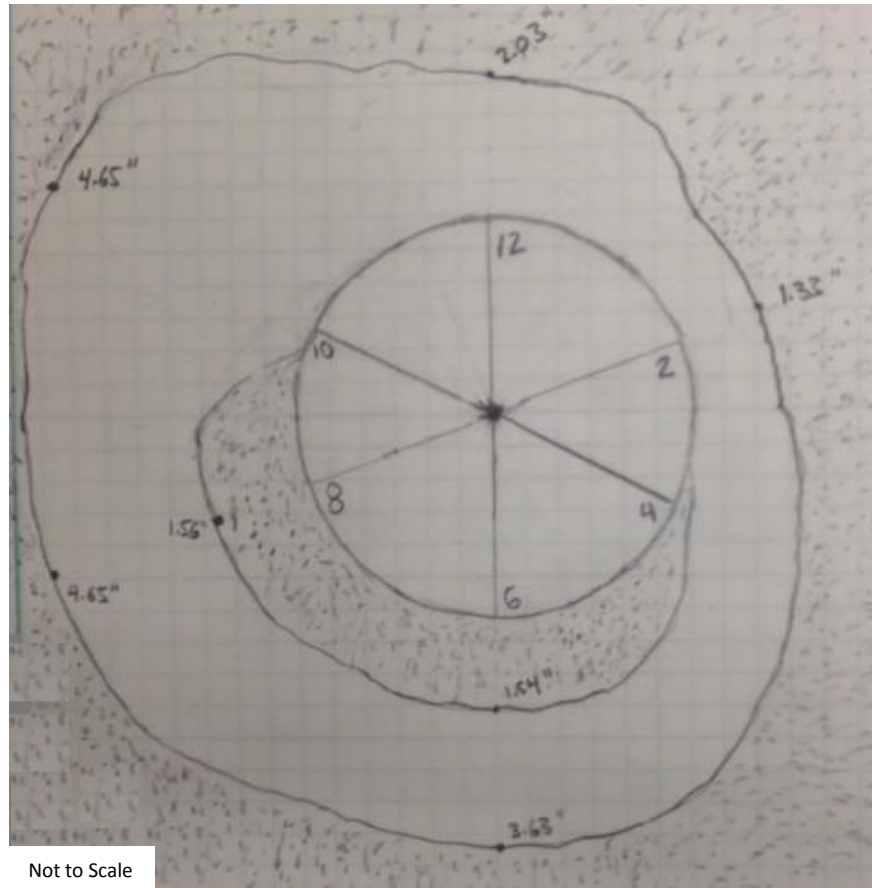
Figure 55. Anomaly detected by FutureScan near the middle of the piping system.

The composition of the anomaly shown in Figure 55 is unknown, but it is unfavorable. Due to high roadway movements (approximately 1-inch), settlement and heave tolerances are almost exceeded. In the long-term, settlements of 0.78-inches and heaves of 1.62-inches occur in or near the anomalous region. Four months after project completion, the roadway yielded surface movement, exceeding that of tolerated settlements and heaves. In the case of Burnt Chimney, once unfavorable results were detected (Figure 55), remediation could have been the next step to construction. Grouting of the annular space would have been a viable remediation option, reducing potential hazardous roadway movement in the future.

FutureScan was not only capable of detecting a critical section of soil around the perimeter of the pipe in a real project setting but was also successful in locating small target voids. Target thicknesses, detected by FutureScan, are deemed accurate to an average value of 0.0925-inches. So, on average, FutureScan can accurately measure void thickness, to +/- 0.10-inches, pertinent to anomalies existing close to the scanner. Table 12 compares actual target thicknesses to FutureScan detected thicknesses.

Table 12. FutureScan Results for target region.

Target Thickness (in.)	CUES Target Thickness (in.)
¼	¼
¼	.32
¼	.29
½	.24

When considering one-dimensional soil consolidation theory, void ratio is the basis for analysis. Primary consolidation is defined by the explusion of voids. Settlement and change in void ratio have a direct relationship: more void explusion is indicative of more settlement. Therefore, with FutureScan's capability to measure thicknesses in the vertical direction, FutureScan can be a vital tool in predicting settlement due to one-dimensional consolidation.

Although FutureScan's thickness detection is excellent close to the pipe wall, error did exist in FutureScan target detection, pertaining to length and location. FutureScan location capability, along the pipe, showed 12.5% error. FutureScan target length capability displayed 16.6% error. FutureScan target thickness capability displayed 21.9% error, but targets were very small: ¼-inch to ½-inch thick. The error, that exists in location or spacing, is due likely due to the manual counting method and misaligment of the spool counter and cable feed. If the actual cable fed from the spool differs from the counter, then differing results will be relayed to the acquistion system. Also, the FutureScan antenna displayed difficulty in measuring targets larger than itself, causing the void length error. Overall, FutureScan had the amazing capability to measure void thicknesses to an an average accuracy of +/- 0.10-inches.

GPR's capability in locating thin voids close to pipe wall surfaces is not deemed reliable, although GPR was capable of detecting a breach in the pipe wall at the VA-635 site. The size of the breach is unknown at this point in time. As a general rule of thumb in the field, GPR can measure 1-inch of void thickness for every 1-foot of depth (Garnto, Jeff (Reed Tech, Inc.), Personal Communication, September 2013). For example, GPR can not generally detect a 1-inch void that exists 2-feet below the ground surface, although it should be capable of detecting a 2-inch void that exists 2-feet below the ground surface. GPR is deemed more reliable when measuring larger void spaces that exist in shallower conditions. This theory is consistent with prior research performed in the field as well as the VA-635 project research.

Chen's research, which was peformed in 2010 with a 400-Megahertz GPR antenna, was capable of detecting anomalies of large thickness: 1.26-feet in thickness founded at a depth of 0.54-feet to 1.80-feet and 6-feet in thickness founded at a depth of 2-feet

to 8-feet (Chen, 2010). GPR consistently detected anomalies at a 1(inch): 1(feet) ratio (thickness: depth) at the VA-635 project site. The 3-inch anomaly detected near the 48-inch PP pipe at the VA-635 site was founded at a depth of 2-feet. The 2-inch thick anomaly detected near the 30-inch PP pipe at VA-635 site was founded at a depth of 2.10-feet. Finally, a 2-inch to 3-inch thick anomaly was detected 1-foot from the asphalt surface in considering the 48-inch PP pipe. Table 13 lists GPR capability with depth: anomalies detected, thicknesses, founding depths, and project details.

Table 13. GPR Anomaly Detection Capability.

Project Site	Pipe Size (in)	Soil Conditions	Founded Depth of Anomaly (feet)	Thickness of Anomaly (inches)	GPR Detectability (Yes/No)
Burnt Chimney	18	Virginia Piedmont (Dirty SANDS)	4-feet →5-feet	0.25 to 0.50	No
VA-635 I.	48, triple-wall	FILL – Crusher Run	2-feet → 2.25-feet	3.0	Yes
VA-635 I.	48, triple-wall	FILL – Crusher Run	1.05-feet → 1.30-feet	2.0 – 3.0	Yes
VA-635 II.	30, double-wall	FILL – Crusher Run	2.10-feet → 2.30-feet	2.0	Yes
U.S. 290 – Austin, T.X.	N/A	Unknown	1.75-feet → 7.75-feet	72.0	Yes
I – 40 – Amarillo, T.X.	N/A	Unknown	0.54-feet → 1.80-feet	15.0	Yes

GPR proved to be a reliable system on the VA-635 project sites. Piping soil covers, ranging from 2 to 2.5-feet, were deemed detectable in granular soils (granites and crusher runs) by the GPR method. GPR was capable of detecting anomalies close to the surface that FutureScan could not. FutureScan's range of detection for the Burnt Chimney site was approximately 8-inches outside pipe walls based on the set sampling rate. The GPR antenna was incapable of receiving signals from deeper depths in the Burnt Chimney dirty sands. On the other hand, GPR was capable of detecting anomalies at least 2-feet below the antenna in the case of the VA-635 (48-inch PP pipe) granites. In comparison, FutureScan was able to detect pipe diameters and breaches of the pipe walls but nothing further, due to water cluttering the signal. Table 14 summarizes the reliability of the non-destructive test methods (GPR and FutureScan) on the three sites.

Table 14. Test Site Conditions and Detectability.

Project Site	Pipe Size (in)	Depth of Cover (feet)	Soil Conditions	Detectability of FutureScan	Detectability of GPR
Burnt Chimney	18	Varies from 5.0 to 8.0	Virginia Piedmont (Dirty SANDS)	~8.0-inches above and below pipe wall	~ 3.15-feet below asphalt surface
VA-635 I.	48, triple-wall	2.0	FILL – Crusher Run	At pipe wall	~ 4.20-feet below asphalt surface
VA-635 II.	30, double-wall	2.5	FILL – Crusher Run	At pipe wall	~ 4.20-feet below asphalt surface

Conclusions

Although FutureScan displayed some error in void target detection, it is a reliable and successful system. The wheel-mounted system has the capability to be inserted into deep piping systems and detect anomalies close to outer wall surfaces. FutureScan did display difficulty in detecting anomalies in wet piping systems. Back-reflected signals from surrounding water produced static signals on the radar gram. As expected, GPR was successful in detecting shallow anomalies in coarse-grained soils (crusher run and granites) at the VA-635 sites. GPR was not successful in detecting target voids deep below the surface at the Burnt Chimney site. With deeper soil covers and utilities in the vicinity, the test GPR is not reliable in detecting voids. The problem could be due to interference since dielectric constant changes were not seen below existing utilities that lie above the 18-inch casing. Below this line, changes in dielectric constant were not detected.

Relative elevations show asphalt surface movement during reaming and after pipe insertion. It is also interesting that FutureScan results show the same region varying considerably in terms of anomaly. The anomaly is likely the annular overcut or has been caused by the annular overcut. Surface variances and FutureScan results indicate this region is highly susceptible to drilling fluid pressure and borehole cutting diameter.

FutureScan was capable of detecting deep voids close to the pipe at the Burnt Chimney project site. This could also be due to measuring origin. The measuring origin is close to the installed anomalies, lying on the outer pipe wall. Simply, deeper piping systems will require the FutureScan method of evaluation; whereas, shallower piping systems may require the GPR method of evaluation. For extremely wet piping systems, FutureScan may require a means of water clutter suppression.

Limitations for the FutureScan technology include the following: Ferrous piping systems, extremely wet piping systems, piping systems that are less than 15-inches in inner diameter, and anomalies that are larger than the scanner in length. The

FutureScan coaxial cable spool must also be checked for quality and accuracy prior to beginning detection. Despite the limitations, FutureScan proves to be the only solution for anomaly detection for deeper piping systems that are dry. FutureScan has proven to be a reliable system for anomaly and void detection with little error association.

Recommendations

A further step in this research would be to use a controlled laboratory setting. Varying soils covers, soils, voids, and pipes would all advance the knowledge of the subject matter. A laboratory setting would allow for more precise threshold determination. Exact thresholds could be determined by moving void systems further and further away from the measuring origin. A similar experiment could be performed with the GPR wheel-mounted system.

FutureScan is also capable of grout detection. An interesting experiment would entail grout detection and grout evaluation around the outer pipe wall. The consistency and thickness of grout around the outer pipe wall could be evaluated with FutureScan. Varying grout slumps and admixtures could indicate whether FutureScan is capable of evaluating grout performance. Voids inside grout could potentially be detected using FutureScan. Since many trenchless projects involve grouting of the annular space, FutureScan could be a great means to evaluating this process.

Acknowledgements

References

ASTM Standard D422, 1963 (2007), "Standard Test Method for Particle-Size Analysis of Soils," ASTM International, West Conshohocken, PA, 2007, DOI: 10.1520/D0422-63R07, www.astm.org.

ASTM Standard D4318, 1983 (2010), "Standard Tests for Liquid Limit, Plastic Limit, and Plasticity Index of Soils," ASTM International, West Conshohocken, PA, 2010, DOI: 10.1520/D4318-10, www.astm.org.

ASTM Standard D6913, 2004 (2009), "Standard Test Methods for Particle-Size Distribution (Gradation) of Soils Using Sieve Analysis," ASTM International, West Conshohocken, PA, 2009, DOI: 10.1520/D6913-04R09.

Bennett, D., (2009). "HDD Design Issues: Hydrofractures," Trenchless Technology – Home. Trenchless Online, Oct. 2012. < http://www.trenchlessonline.com/index/webapp-stories-action/id.697>.

Chen, D.H. (2010). "Using Ground-Coupled Radar Techniques to Detect Concealed Subsurface Voids," Texas Department of Transportation: Construction and Bridge Divisions (Copyright September 2010), Austin, TX.

Francis, M., Kwong, J., and Kawamura, K., (2003). "Analysis of Heave and Subsidence Risk for Horizontal Directional Drilling," ASCE Pipeline 2003 (Copyright 2004), Honolulu.

Gelinas, Marc M. and Mathy, David C. (2004). "Designing and Interpreting Geotechnical Investigations for Horizontal Directional Drilling," ASCE Pipeline 2004 (Copyright 2004), San Diego, CA.

Grazzini, G., Pieraccini, M., Parrin, F., and Atzeni, C. (2007, June). "A Clutter Canceller for Continuous Wave GPR," Advanced Ground Penetrating Radar, 2007 4th Workshop on, IEEE, 2007.

Hashash,Y. and Javier, J., (2011). "Evaluation of Horizontal Directional Drilling (HDD)," Illinois Center for Transportation, Report No. FHWA-ICT-11-095, Nov. 2011.

Hoppe, E.J., (2011). "Evaluation of Polypropylene Drainage Pipe," Virginia Center for Transportation Innovation and Research, Final Report VCTIR 11-R14, Dec. 2013. <http://www.virginiadot.org/vtrc/main/online_reports/pdf/11-r14.pdf>.

Iseley, T. and Gokhale, S., (1997). "Synthesis of Highway Practice 242 – Trenchless Installation of Conduits Beneath Roadways," Transportation Research Board --

National Cooperative Highway Research Program, National Academy Press, Washington , D.C. 1997.

J.D. Hair & Associates, Inc., et. al. (1995). "Installation of Pipelines by Horizontal Directional Drilling – An Engineering Design Guide," Pipeline Research Committee, American Gas Association.

Nathanson, F.E., Radar Design Principles. New York: McGraw-Hill, 1969.

United States Geological Survey (USGS) National Map – Home. USGS, Nov. 2013. Web. 03 Dec. 2013. <http://nationalmap.gov/viewer.html>.

Wightman, W.E. Jalinoos, F., Sirles, P., and Hanna, K. (2003). "Application of Geophysical Methods to Highway Related Problems." Federal Highway Administration, Central Federal Lands Highway Division, Lakewood, CO, Publication No. FHWA-IF-04-021, September 2003. <http://www.cklhd.gov/resources/agm>.

Web Soil Survey - Home. Web Soil Survey - Home. USDA, 15 Feb. 2013. Web. 03 Dec. 2013. <http://websoilsurvey.sc.egov.usda.gov/App/HomePage.htm>.

Yestrebsky, Tom and Winiewicz, Tony (2013). "Virginia Department of Transportation Trial Customer Report – Interim Report." CUES, Inc, Orlando, FL, December 2013.